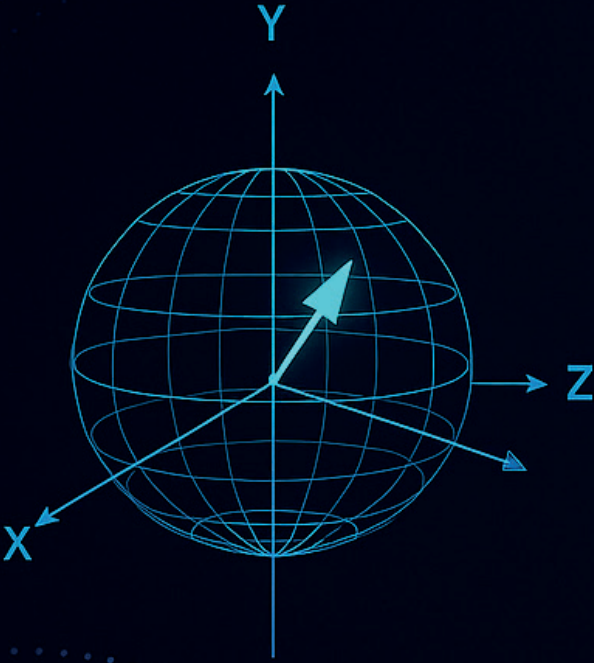




# Journal of Quantum Technologies and Informatics Research

International Peer-Reviewed and Open Access Electronic Journal

Uluslararası Hakemli ve Açık Erişimli Elektronik Dergi

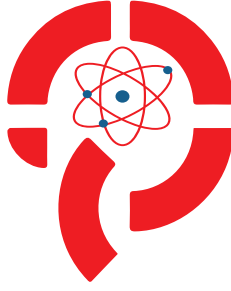


Quantum-Enhanced Conformal  
Methods for Multi-Output  
Uncertainty: A Holistic Exploration  
and Experimental Analysis

Davut Emre Tasar







Journal of Quantum Technologies  
and Informatics Research

**JQT/IR**

E-ISSN: 3023-4735

DOI: 10.70447/ktve

International Peer-Reviewed and Open Access Electronic Journal  
Uluslararası Hakemli ve Açık Erişimli Elektronik Dergi

Volume/Cilt: 3

Issue/Sayı: 1

Year/Yıl: 2025

E-posta: jqtair@gmail.com

Web: <https://journals.gen.tr/index.php/jqtair/>

İletişim: Adres: Anafartalar Yerleşkesi, B2 Blok, Oda No: 8,  
Çanakkale, Türkiye



**HOLISTENCE**  
publications

*“This page is left blank for typesetting”*



**HOLISTENCE**  
publications

*Bu sayfa dizgiden dolayı boş bırakılmıştır*

## EDITÖR'den

### 2025 Mart Sayısı – Sürekli Yayın Dönemi Başlıyor

Bilimin sınırlarını genişletmek, yalnızca bilgi üretmekle değil, bu bilgiyi zamanında, erişilebilir ve etkin biçimde paylaşmakla mümkündür. *Kuantum Teknolojileri ve Enformatik Araştırmaları Dergisi* (KTEAD / *Journal of Quantum Technologies and Informatics Research - JQTAIR*) olarak siz değerli okuyucularımızla 2025 **Mart** sayımızı paylaşmanın heyecanını yaşıyoruz. Bu sayımız, hem içerik yönüyle hem de yayın politikası açısından yeni bir dönemin başlangıcını simgelemektedir.

### Sürekli Yayın Modeline Geçiş

Bu sayıdan itibaren dergimiz, akademik dünyada giderek yaygınlaşan ve erişimi hızlandıran “**Sürekli Yayın / Continuous Publishing**” modeline geçmiştir. Artık her makale, hakem süreci tamamlandıktan hemen sonra çevrim içi erişime açılacak ve sayı tamamlanmadan da atıf alabilir hâle gelecektir. Bu geçişin temel motivasyonu, yazarlarımızın katkılarını daha kısa sürede bilimsel dolaşıma kazandırmak ve okuyucularımıza da güncel bilgiye hızlı erişim sağlamaktır. Ayrıca bu model, araştırma çıktılarını zaman kaybetmeden görünür kıldığı için, atıf potansiyelini de artırmaktadır.

### Uluslararası Başarılarımız

2025 yılı itibariyle dergimiz, **çok sayıda saygın uluslararası indeks** tarafından taranmaya başlamış, böylece sadece Türkiye’den değil, Avrupa’dan Asya’ya birçok araştırma merkezinden makale başvuruları almaya başlamıştır. Bu durum, KTEAD’in bilimsel tutarlılık, hakemlik disiplini ve konu odaklılığı açısından güvenilir bir kaynak hâline geldiğini göstermektedir.

### Öne Çıkan Çalışma: Kuantum Belirsizliğe Yeni Bir Yaklaşım

Bu sayımızda özellikle dikkat çeken çalışmalardan biri, **Davut Emre Taşar** tarafından kaleme alınan ve *University of Navarra* kökenli olan “**Quantum-Enhanced Conformal Methods for Multi-Output Uncertainty**” başlıklı makaledir. Bu çalışmada, klasik konformal tahmin yaklaşımlarının, çok boyutlu kuantum olasılık dağılımları üzerindeki etkisi deneysel olarak incelenmiş; 2-qubit sistemlerin farklı ölçüm bazlarındaki belirsizlikleri nasıl kapsayabileceği ileri düzey bir yöntemle analiz edilmiştir.

Makale, klasik rastgele orman regresörleri ile kuantumdan türetilen çok çıkışlı (multi-output) verileri ilişkilendirmekte ve bu ilişki üzerinden dağılımsız güven aralıkları üretmektedir. Taşar’ın önerdiği **kuantum-konformal hibrit model**, hem teorik çerçevesi hem de açık kaynak kodlarla desteklenen uygulama düzeyi ile alanında öncü niteliktedir. Özellikle Z, X ve Y bazlarındaki ölçüm olasılıklarının 12 boyutlu uzayda modellenmesi, geleceğin kuantum yapay zekâ uygulamaları için bir temel teşkil etmektedir.

### TÜBİTAK UME'den Yenilikçi Bir Katkı: Kuantum Gerilim Standardı

Bu sayının bir diğer dikkat çekici makalesi, **TÜBİTAK Ulusal Metroloji Enstitüsü (UME)** bünyesinde gerçekleştirilen öncü bir çalışmadır: “**Kriyojenik Soğutucuda Çalışan Kuantum Programlanabilir Gerilim Standardının Kurulumu**”

Bu çalışma, Türkiye’de kuantum ölçüm sistemlerinin altyapısal anlamda inşasına yönelik atılan en somut adımlardan biridir. Özellikle Josephson etkisine dayalı gerilim standartlarının, kriyojenik soğutucularla entegre edilerek stabil ve tekrar üretilebilir gerilim değerleri üretmesi; yalnızca temel bilimler için değil, aynı zamanda kalibrasyon, elektriksel metroloji ve sanayi tabanlı hassas ölçüm uygulamaları için de hayati bir adımdır.

---

Bu makale, yalnızca teknik yeterliliğiyle değil, aynı zamanda **Türkiye'nin kuantum metrolojisi alanında uluslararası normlara entegre olma çabasının da bir yansıması** olarak okunmalıdır. KTEAD olarak bu tür altyapı temelli makalelere kapımız her zaman açıktır.

### **Multidisipliner Yaklaşım ve Akademik Derinlik**

2025 Mart sayısında yer alan diğer çalışmalar da, kuantum teknolojileri ile enformatik sistemlerin kesişim kümesinde yer alan kritik sorunları incelemektedir. Bu sayede, bir yandan **kuantum hesaplama, belirsizlik modelleme, hibrit veri işleme**, öte yandan **makine öğrenmesi ile ticari karar alma** gibi alanlar arasında köprü kurulmaktadır.

Bu yaklaşım, dergimizin yalnızca bir fizik ya da mühendislik dergisi değil, **yenilikçi bilgi sistemlerini kuantum paradigmasıyla yeniden yorumlayan bir araştırma platformu** olduğunu da göstermektedir.

### **Gelecek Vizyonumuz**

KTEAD olarak vizyonumuz; sadece yayın yapmak değil, **bir bilimsel topluluk inşa etmektir**. Kuantum teknolojileri gibi hızla gelişen bir alanda; etik yayıncılık ilkelerine bağlı, disiplinler arası etkileşimi teşvik eden ve özgünlüğü ön planda tutan bir yayın politikasıyla ilerlemeye devam edeceğiz.

Önümüzdeki sayılarda, kuantum donanımlar, kuantum algoritmalar, kuantum iletişim güvenliği ve kuantum-yapay zekâ etkileşimi konularında daha fazla sayıda nitelikli çalışmayı görmekten memnuniyet duyacağız.

Bu vesileyle, katkı sunan yazarlarımıza, titiz değerlendirmeleriyle süreci şeffaflaştıran hakemlerimize, editör yardımcısı ve yayın kurulu üyelerimize teşekkür ederim.

Bilimin yayını gecikmemeli. Bu nedenle sürekli yayın yapısına geçerken, siz değerli araştırmacıların desteğiyle kuantum çağının öncü yayınlarından biri olmayı sürdüreceğiz.

Saygılarımla

**Dr. Cumali YAŞAR**

**Editör**

*Kuantum Teknolojileri ve Enformatik Araştırmaları Dergisi (JQTAIR)*

**2025 / Mart – Sürekli Yayın İlk Sayı**

---

## From the EDITOR

### March 2025 Issue – Transition to Continuous Publishing

Scientific progress depends not only on the production of knowledge but also on the timely, accessible, and efficient dissemination of that knowledge. As the *Journal of Quantum Technologies and Informatics Research* (JQTAIR / *Kuantum Teknolojileri ve Enformatik Araştırmaları Dergisi* – KTEAD), we are pleased to share with you the March 2025 issue, which marks the beginning of a new era both in terms of content and editorial policy.

### Transition to Continuous Publishing

As of this issue, JQTAIR has officially adopted the **Continuous Publishing Model**. Under this model, accepted articles are published online immediately after the peer review and editorial processes are complete—without waiting for the full issue to be compiled. This shift is motivated by our commitment to ensuring that valuable research is **shared promptly** with the global scientific community. It also enhances the **citation potential** of articles by making them discoverable sooner.

### A New Phase of International Recognition

Our journal has now been included in **numerous prestigious international indexes**, reflecting the quality, consistency, and scientific rigor of our publications. We are proud to note a significant increase in submissions from a wide range of countries—from Turkey to Europe, Asia, and beyond—further confirming JQTAIR’s position as a trusted platform in the field.

### Highlight Article: A Quantum Leap in Uncertainty Modeling

Among the standout contributions in this issue is the article by **Davut Emre Taşar**, titled “**Quantum-Enhanced Conformal Methods for Multi-Output Uncertainty: A Holistic Exploration and Experimental Analysis**”, submitted from the University of Navarra.

In this groundbreaking work, the author successfully integrates **classical conformal prediction methods with quantum-generated, high-dimensional probability distributions**. By leveraging classical multi-output regression models and conformal calibration techniques, Taşar demonstrates how reliable uncertainty quantification can be achieved even when the underlying data is inherently quantum.

Notably, the article explores the use of 2-qubit circuits measured in Z, X, and Y bases, yielding 12-dimensional outputs. These are modeled with classical regressors and then evaluated via distribution-free conformal prediction—setting a new benchmark for **hybrid quantum-classical machine learning**. The author also provides **open-source code and reproducible Colab notebooks**, ensuring transparency and usability across the research community.

### TÜBİTAK UME’s Contribution: A Milestone in Quantum Voltage Standards

Another remarkable contribution in this issue comes from the **National Metrology Institute of Turkey (TÜBİTAK UME)** with the article titled: “**Development of a Programmable Josephson Voltage Standard Operating in a Cryogenic Refrigerator**”.

This paper details the development of a **quantum voltage standard system** based on the Josephson effect, integrated within a **cryogen-free refrigeration system**. The importance of this work lies not only in its technical precision but also in its role in **building national infrastructure for quantum electrical metrology**—bringing Turkey closer to international quantum measurement standards.

Such systems are essential for calibration, precision instrumentation, and quantum-enabled industrial applications, and this work represents a significant step forward in localizing cutting-edge measurement technologies.

### **Multidisciplinary Scope and Research Depth**

This issue also presents several other high-quality studies that reflect the rich intersection between **quantum technologies and informatics**. Topics include quantum computing, hybrid data modeling, machine learning for decision-making, and experimental quantum algorithms.

This multidisciplinary range reinforces JQTAIR's mission to serve as not just a physics or engineering journal, but a **cross-disciplinary platform exploring the informatic and computational aspects of quantum science**.

### **Looking Ahead**

At JQTAIR, our vision extends beyond publishing—it is about building a scientific **community of collaboration and trust**. As quantum science rapidly evolves, we remain committed to upholding ethical standards, promoting rigorous peer review, and fostering innovation across disciplines.

In future issues, we look forward to welcoming more contributions in areas such as quantum algorithms, secure quantum communication, quantum-enhanced artificial intelligence, and hardware-embedded quantum technologies.

I extend my sincere gratitude to all contributing authors, dedicated reviewers, editorial board members, and institutional supporters. Your work ensures that we not only maintain the journal's scientific integrity but also continue to elevate its global reach.

As we launch this **first issue under the Continuous Publishing model**, we reaffirm our mission: **to support researchers in making their work visible without delay** and to stand at the forefront of quantum and informatics research.

With kind regards,

**Dr. Cumali YAŞAR**

Editor-in-Chief

*Journal of Quantum Technologies and Informatics Research (JQTAIR)*

**March 2025 – First Continuous Issue**

# EDITORS/EDİTÖRLER

## **Sahibi ve Yayıncı**

Dr. Cumali YAŞAR

## **Editör**

Dr. Cumali YAŞAR

## **Yayın Kurulu**

*Prof. Dr. İdris KABALCI*

*Prof. Dr. Eden Mamut*

*Prof. Dr. Emin Uğur ULUGERGERLİ*

*Prof. Dr. Mehmet ŞAHİN*

*Prof. Dr. Mehmet Emin ÖZEL*

*Doç. Dr. Can AKTAŞ*

*Doç. Dr. Uğur ERCAN*

*Dr. Öğr. Üyesi Sevdanur GENÇ*

*Dr. Öğr. Üyesi Bayram KÖSE*

*Dr. Öğr. Üyesi Ahmet Zahid KÜÇÜK*

*Dr. Öğr. Üyesi Sevgi DEMİRCİOĞLU*

*Dr. Ceren ÖCAL TAŞAR*

*Dr. Öğr. Üyesi Samet MEMİŞ*

*Öğr. Gör. Dr. Cumali YAŞAR*

*Dr. Öğr. Üyesi Veli Özcan BUDAK*

*Dr. Ali ÇİMEN*

## **Teknik Destek**

*Cumali Yaşar*

## **Dergi Tasarımı**

*İlknur Hersek Sarı*

**İletişim:** Anafartalar Yerleşkesi,

B2 Blok, Oda No: 8, Çanakkale, Türkiye

Telefon: 5052423644

E-posta: jqtair@gmail.com

Web: <https://journals.gen.tr/index.php/jqtair/>



# CONTENTS / İÇİNDEKİLER

Baş Editörden | III

RESEARCH ARTICLE / ARAŞTIRMA MAKALESİ

Establishing of Quantum Voltage Standard in Cryogenic Cooler at TÜBİTAK UME | 1

*TÜBİTAK UME'de Kriyojenik Soğutucuda Kuantum Gerilim Standardının Kurulumu*

**Mehedin Arifoviç & Naylan Kanatoğlu & Recep Orhan**

RESEARCH ARTICLE / ARAŞTIRMA MAKALESİ

Why E-Commerce Startups Fail: Can machine learning provide solution? | 1

**Mona Yadegar**

RESEARCH ARTICLE / ARAŞTIRMA MAKALESİ

Quantum-Enhanced Conformal Methods for Multi-Output Uncertainty: A Holistic Exploration and Experimental Analysis | 1

**Davut Emre Tasar**

*“This page is left blank for typesetting”*



**HOLISTENCE**  
publications

*Bu sayfa dizgiden dolayı boş bırakılmıştır*

# Establishing of Quantum Voltage Standard in Cryogenic Cooler at TÜBİTAK UME

## TÜBİTAK UME'de Kriyojenik Soğutucuda Kuantum Gerilim Standardının Kurulumu

Mehedin Arifoviç<sup>1</sup>  Naylan Kanatoğlu<sup>2</sup>  Recep Orhan<sup>3</sup> 

<sup>1</sup>TÜBİTAK, Ulusal Metroloji Enstitüsü, Gebze, Kocaeli, Türkiye, e-mail: Mehedin.arifovic@tubitak.gov.tr

<sup>2</sup>TÜBİTAK, Ulusal Metroloji Enstitüsü, Gebze, Kocaeli, Türkiye, e-mail: naylan.kanatoglu@tubitak.gov.tr

<sup>3</sup>TÜBİTAK, Ulusal Metroloji Enstitüsü, Gebze, Kocaeli, Türkiye, e-mail: recep.orhan@tubitak.gov.tr

### Abstract

This paper describes the implementation of a programmable Josephson voltage standard in a cryogenic cooler at the National Metrology Institute of Türkiye (TÜBİTAK Ulusal Metroloji Enstitüsü). This work includes the installation of a 10 V Josephson array in the cryostat, installing the devices necessary for its operation, preparing software for system control and optimization, and testing the installed system.

**Keywords:** Josephson effect, PJVS, Voltage standard, Metrology, SI system

### Öz

Bu makalede, TÜBİTAK Ulusal Metroloji Enstitüsü'ndeki kriyojenik soğutucuda programlanabilir bir Josephson gerilim standardının kurulumu anlatılmaktadır. Bu çalışma, 10 V Josephson dizisinin kriyojenik soğutucuda montajını, dizinin çalışmasını sağlayacak cihazların kurulumu, sistemin kontrolü ve optimizasyonu için yazılımların hazırlanmasını ve kurulan sistemin test edilmesi sürecini içermektedir.

**Anahtar kelimeler:** Josephson etkisi, PJVS, Gerilim standardı, Metroloji, SI sistemi

Citation/Atf: ARIFOVIC, M, KANATOĞLU, N. & ORHAN, R. (2025). Establishing of Quantum Voltage Standard in Cryogenic Cooler at TÜBİTAK UME. *Kuantum Teknolojileri ve Enformatik Araştırmaları*. 3(1): e2743, DOI: 10.70447/ktve.2743

Corresponding Author/ Sorumlu Yazar:  
Mehedin Arifoviç  
E-mail: Mehedin.arifovic@tubitak.gov.tr



Bu çalışma, Creative Commons Atif 4.0 Uluslararası Lisansı ile lisanslanmıştır.  
This work is licensed under a Creative Commons Attribution 4.0 International License.

## 1. INTRODUCTION

Quantum voltage standards are intrinsic standards based on the Josephson Effect and produce voltages defined solely by the ratio of natural constants: Planck's constant  $h$ , the electron charge  $e$ , and frequency [1]. These are known as Josephson Voltage Standards (JVS), and they have been continuously improved over the past four decades, significantly increasing the accuracy of electrical measurements.

Earlier standards, known as conventional standards, were only suitable for DC voltage due to the hysteretic behavior of junctions in Josephson arrays. Recently, substantial efforts have been made to improve these standards so that they can also be used for AC voltage. However, the practical realization of AC voltage is still based on the calorimetric method, which cannot meet all the requirements of modern measurement technology. As a result, two types of Josephson arrays/systems have been developed: the Programmable JVS (PJVS), which can produce step-approximated AC voltages [2] [3], and the pulse-driven JVS, which can produce pure sine waves up to MHz frequencies, also known as the Josephson Arbitrary Waveform Synthesizer (JAWS) [4][5].

TÜBİTAK UME, as the legal scientific authority for national measurement standards in Türkiye, adopted a conventional 10V JVS in 1997 [6] and demonstrated its expertise through several international comparisons [7].

The increasing demand for dynamic measurements and participation in international collaborations led TÜBİTAK UME to initiate a project to establish a PJVS capable of meeting emerging needs. Although such a standard can be purchased today, the manufacturer's built-in software, designed for basic system functions, makes it nearly impossible to use for more complex measurements that typically involve synchronization with external devices. One example is the UME Kibble Balance [8], a complex system in which the PJVS is a subsystem that must be synchronized with other subsystems. To have full control over the process, a unique PJVS with customizable software was designed to meet

the specific needs of the Kibble balance setup [9]. This system uses liquid helium to provide the cryogenic environment for Josephson array operation.

As part of this project, the implementation of another UME PJVS is planned, which will be optimized for the calibration of semiconductor voltage standards and the testing of digital converters. Although more challenging, it was decided to build the new system into a cryogenic cooler (or cryocooler) due to practical difficulties in using liquid helium and the growing availability of cryogenic cooler technology.

The following paragraphs present the details of the construction and testing of the new system.

## 2. SYSTEM DESCRIPTION

The main components of the UME PJVS in cryocooler (CPJVS) are: Josephson Array, bias electronics, cryogenic system, and software. Details of each component are given below.

### 2.1. Josephson Array

The Josephson array is produced by Supracon AG [10] and has the basic characteristics given in Table 1. The array is fabricated using NbSiX technology with Superconductor-Normal Metal-Superconductor (SNS) layers and contains 69,630 Josephson junctions (JJs) subdivided into 18 segments with a nearly binary sequence.

**Table 1.** Characteristics of the PJVS Array

Parameter	Value
Number of Josephson Junctions	69630
Operating Frequency	69,6 GHz
Maximum Output Voltage	$\pm 10,02$ V
Bias Current	3,1 mV
1 <sup>st</sup> Shapiro Step Width	1 mA
Resolution	144 $\mu$ V (17 bit)
Operating temperature	3,7 K

Figure 1a shows the array, with a small antenna on the right for receiving microwave energy. The array is glued to a small board that has the bias current input connections. During operation, the array generates more than 100 mW of heat, which is not critical when operating in liquid helium but is quite important for array operation in the

cryocooler. To maximize heat transfer between the array and the cryocooler cold stage, a special thermal interface [11] was installed by the array provider (Figure 1b).

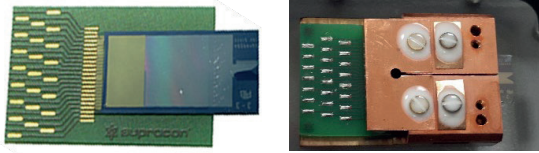


Figure 1. Josephson Array (a) with Thermal Interface (b)

## 2.2. Cryogenic Cooler

### 2.1.1. Cryocooler Setup

The CPJVS array is cooled by a customized closed-cycle, two-stage pulse tube cooler (PTC) from TransMIT GmbH [12]. The PTC is driven by a 7 kW air-cooled CSA-71A Helium compressor, which requires a three-phase 200 V power supply provided through a special three-phase transformer. The available cooling power is approximately 700 mW at 4,2 K and 500 mW at 3,7 K, the operating temperature of the CPJVS array. The power input to the compressor is around 6,5 kW. Due to noise and heat released during operation, the compressor is installed in a separate room. The temperature of the first stage is 44 K, and the second stage achieves 2,2 K without load. The cold stage temperature increases slightly after installing the array and its wiring. Optimum array operation requires a stable temperature. The cryocooler used dampens the intrinsic temperature oscillations caused by the periodic compression/expansion of the Helium working gas in the PTC by condensing liquid helium into the pot installed at the second stage. As a result, the peak-to-peak temperature oscillations at the array carrier are dampened by about 10 mK, providing sufficient working margins.

The cooler is equipped with three temperature sensors and two heaters, which are used in conjunction with the Lakeshore 335 temperature controller to set the proper operating temperature.

### 2.1.2. Installation and Wiring of the Array in the Cryocooler

The array is mounted to the second stage of the cooler on a special finger designed to fit the thermal interface of the array, shown in Figure-2. The interface is screwed onto the finger, and the thermal contact between the finger and the interface is ensured by a layer of Apiezon N grease [13].

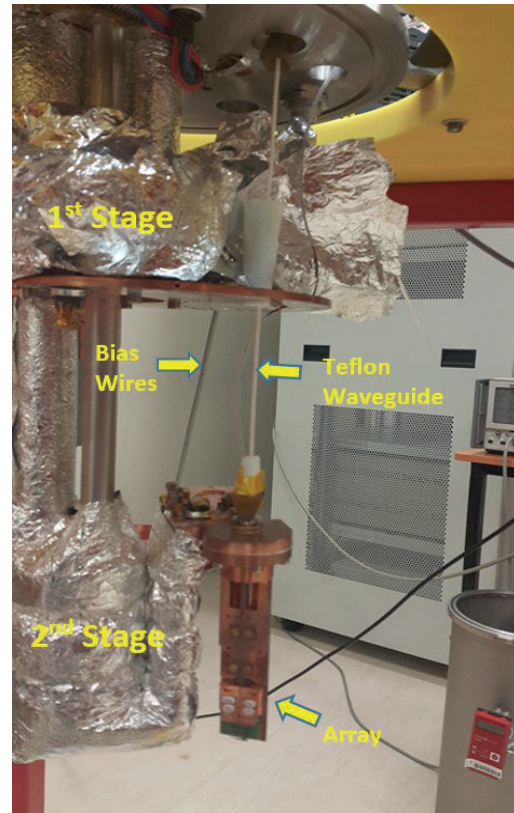


Figure 2. Array and Wiring Inside the Cryocooler

To block the inflow of heat from the outside, the electrical connections to the bias source are made with insulated manganin wires (0,125 mm diameter), tightly twisted together. The voltage output from the chip is made with a twisted pair of thin isolated copper wires (40  $\mu$ m diameter). All wires are thermally anchored to the surfaces of the first stage. Microwave bias is transferred to the array via a Teflon waveguide inserted between the WR-12 waveguide line using two horn antennas [14]. The finger with the array is magnetically shielded with a Cryoperm cylinder cup. Finally, the second stage with the array is protected by a copper cylinder wrapped in several layers of Mylar foil to ensure maximum protection from thermal radiation.

All connections from the array to the outside are made via vacuum-proof connectors on the top side of the cooler chamber. For the WR-12 microwave connector, a window is made from a thin epoxy layer that can sustain a vacuum of  $10^{-5}$  mbar under microwave radiation.

### 2.3. Bias Electronics

For the PJVS to operate properly, two signals need to be fed into the array: an RF microwave signal with a known frequency to produce a reference voltage, and a bias current to ensure that the array operates in a flat quantum region.

#### 2.3.1. Current Bias

As already mentioned, the array used has 18 segments in series, each of which is independent. When biased, each segment produces a voltage proportional to the number of its Josephson junctions. The total voltage produced by the array is the sum of the voltages from all the biased segments.

For current biasing, a National Instruments PXIe-6738<sup>1</sup> 32-channel board, mounted in the NI 1082DC PXI chassis, is used. Since this device operates in voltage mode, it is necessary to know the resistance of each segment's path in order to calculate the voltage that produces the required current. As this board has very low source resistances (0,2  $\Omega$ ), additional resistors were added to each segment's path to keep the applied voltages within regions where the board is more stable. The resistors used have very low inductance, ensuring a fast transition of applied voltages, which is especially important when the PJVS operates in AC mode. Measurements with a high-speed oscilloscope show that the transition time between two voltage steps of this setup is below 2  $\mu$ s. The resistors are placed in an isothermal box to ensure the stability of the applied current. The array's segment parameters and the total resistance of the connecting paths are given in Table 2.

<sup>1</sup> Commercial instruments are identified in this paper in order to adequately specify the experimental procedure. Such identification does not imply recommendation or endorsement by TÜBİTAK UME

**Table 2.** Array Parameters

Segment	JJs	Resistance( $\Omega$ )	Voltage @ 69,6 GHz Bias
1	34.814	35,3	5,01047390 V
2	17.408	111,36	2,50538087 V
3	8.704	111,42	1,25269044 V
4	4.352	110,89	0,62634522 V
5	2.176	110,83	0,31317261 V
6	1.088	111,25	0,15658630 V
7	544	111,31	7,8293152 mV
8	272	111,15	3,9146576 mV
9	136	111,06	1,9573288 mV
10	1	111,84	143,9212 $\mu$ V
11	1	110,91	143,9212 $\mu$ V
12	1	111,13	143,9212 $\mu$ V
13	2	111,10	287,8424 $\mu$ V
14	4	111,30	575,6849 $\mu$ V
15	8	111,49	1,151370 mV
16	17	111,53	2,446661 mV
17	34	111,94	4,893322 mV
18	68	111,07	9,786644 mV

The bias system is isolated from ground by powering the PXI chassis with a battery, and its communication with the computer is achieved via a fiber-optical connection.

#### 2.3.2. Microwave Bias

Microwave bias is provided by a compact synthesizer produced by the TeraHertz Laboratory, a branch of the TÜBİTAK MAM Institute [15]. The synthesizer can produce up to 200 mW of CW power at frequencies between 69 and 71 GHz, with a resolution of 4 kHz. It is locked to a rubidium frequency standard and controlled by the PC via an isolated RS-232 link. To avoid introducing unnecessary energy into the system, it has been determined that 90 mW is the minimum power the synthesizer should send for optimal array operation. Approximately 40 mW is directly radiated into the array, and the rest is dissipated or reflected along the microwave path.

### 2.4. Software

The control software is developed using the NI LabVIEW platform. It features several windows with an intuitive graphical user interface,

providing the user full control over the system. The main window, "Array Parameters," allows users to set all array parameters, such as the number of segments, the number of Josephson junctions (JJ) in each segment, path resistances, and bias currents. There is also a function that automatically measures the bias current of all segments, but the user also has the option to optimize this parameter manually.

For any selected output voltage of the CPJVS, the program automatically calculates the voltages applied to all 18 bias channels of the array, based on the microwave frequency and array parameters. The output voltage is measured by a high-resolution voltmeter, Keysight 3458A, which is connected to the computer via the GPIB interface.

The user can also access other windows for measurement procedures, such as calibrating a DC voltage standard or determining the linearity of a high-resolution voltmeter. In addition, there are specific subprograms for AC applications, which are more specialized and depend on the instrument under test and its synchronization capabilities with the PJVS.

It should be noted that the UME CPJVS supports clock-in and trigger-out connections with external devices, which is included in each of the specific programs.

## 2.5. System Operation

The complete system is shown in Figure 3. Before operating the cryocooler, the vacuum chamber with the built-in cold stages is pumped to a pressure of less than  $10^{-3}$  mbar. The cryocooler reaches its final temperature of about 3 K in approximately 8 hours. The cooling process can be monitored through the software, which records the cooling chart.

Once the system has cooled down, the bias electronics are powered on, the software is started, and the system is optimized for operation. This includes tuning the RF generator and determining the optimal bias currents for each segment. When the array enters the optimal operating mode, its I-V characteristics are as shown in Figure 4 (for segments 4-8, for clarity).

The flat voltage regions correspond to the quantum-defined voltages of each segment. The widths of the bias currents that induce quantum voltage are important parameters, as they indicate the operating margins of the system.



**Figure 3.** UME CPJVS

In the UME CPJVS, these currents range from 0,6 mA for the four largest segments to about 1 mA for the smaller ones. The bias currents, which are set to the middle of the quantum voltage regions in the software, act as the operating points for each segment. These currents cluster around 3,1 mA, with a maximum variation of 0,3 mA, depending on the segment, which is consistent with the manufacturer's specifications for the array. The optimal bias currents generally do not change during the same cryogenic operating cycle, and any changes are more likely related to trapped currents (or flux) within the array. This phenomenon occurs when external electrical noise is injected into the chip while it is in the superconducting state via cables. It usually manifests as very narrow or non-existent flat voltage regions in the I-V characteristics of one or more segments.

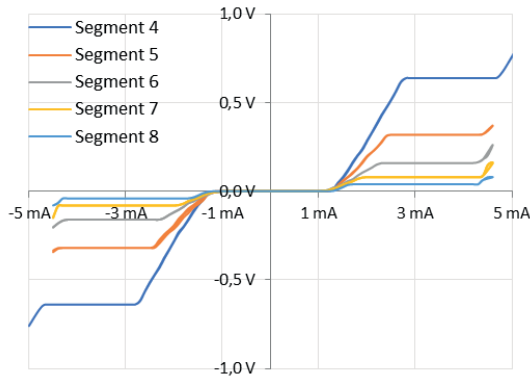


**Figure 4.** I-V characteristics of Segments 4-8

In such cases, the array can be heated to exit the superconducting state using the temperature controller and heater installed between the first and second cooling stages. When the temperature sensor on the second stage reads 12 K, maintaining this temperature for about 10 minutes is sufficient to clear the trapped current.

Once the bias currents are optimized, the system is ready for use. In the first stage, a high-resolution voltmeter is used to test the system at several voltages. During this process, the optimal bias currents are deliberately varied (dithered) to confirm that the chip is operating in the quantum regime. This practice is also applied for other measurements. If it is observed that the width of the voltage step is below the specified criterion, the chip heating procedure is performed.

### 3. SYSTEM TEST

#### 3.1. DC Voltage

As previously mentioned, TÜBİTAK UME has been using a DC conventional JVS since 1997, proven in several international comparisons. These comparisons typically use a DC standard with a known drift as a traveling standard. The UME CPJVS was compared to the existing system using the same approach. For comparison, a Fluke 732B DC standard, calibrated periodically with the UME JVS for over 25 years, was used. This ultra-stable DC source has outputs of 1,018 V and 10 V. During the measurement, the DC standard is connected in reverse series with the UME CPJVS, adjusted as close as possible to the DC standard output, and their difference is measured using a Keithley 2182A nanovoltmeter.

To remove offsets and thermal voltages in the loop, the measurement is performed in two stages, forward and reverse polarity mode. A special low-thermal switch is used to connect the DC standard, which has a fixed polarity, unlike the CPJVS, which can be easily reversed by software. The actual output of the DC standard is calculated as the sum of the CPJVS voltage and the measured difference. The measurement results show that the difference between the measured and predicted value at 10 V is about 20 nV, which is far below the uncertainty of the DC standard calibration. The excellent agreement between the two systems can be seen in Figure 6, which shows the long-term drift trend of the DC standard along with the measurements of both systems.

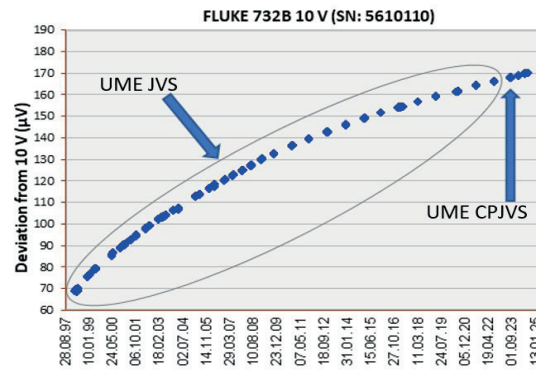


**Figure 5.** Long-term Drift of the DC Standard

#### 3.2. AC Voltage

PJVS systems can generate voltages very quickly due to their non-hysteretic array. This feature allows for the creation of time sequences of voltages with arbitrary shapes, which requires synchronization and timing of all segments of the array, i.e., bias channels. As previously mentioned, the UME CPJVS uses a multichannel board as a bias current source, and all channels are synchronized directly on the board. Additionally, the board can be synchronized with external devices through timing and trigger connections.

The rms accuracy of the PJVS synthesized signals is limited by the transition time between steps, which depends on the wiring and bias electronics. However, the steps of the generated waveform are intrinsic quantum voltages and are suitable for use with digital converters. As

an example, the synthesis and application of a sine signal, commonly used in AC applications, is shown here.

### 3.2.1. System Description

Figure-7 shows the schematic of the system used for testing a digitizer (Keysight 3458A) in dynamic mode using the UME CPJVS.

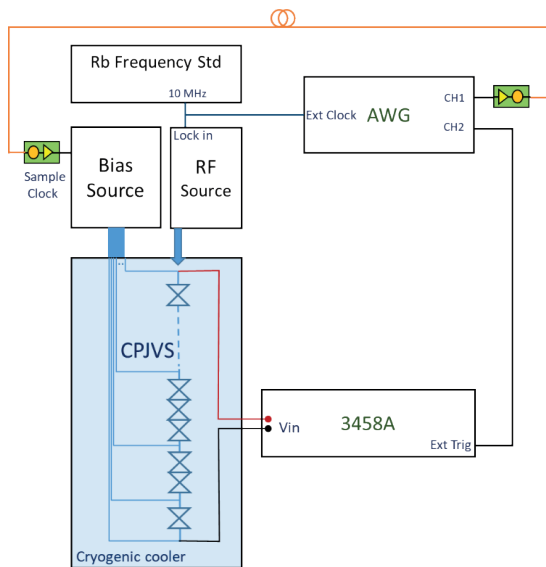


**Figure 6.** System for Testing Digitizer Using UME CPJVS

The digitizer used has a 28-bit integrative DAC and allows full control over its measurement functions, such as resolution, timing, and sampling parameters. It is synchronized to the UME CPJVS using an arbitrary waveform generator (AWG) locked to a rubidium frequency standard. The other channel of the AWG is connected to the CPJVS bias source via fiber-optic electro-optical converters to keep the system in floating mode.

### 3.2.2. Measurement Procedure

The test signal applied by the CPJVS is a 20-step approximated sine wave with a 2 V<sub>pp</sub> amplitude at a frequency of 62,5 Hz. The system software automatically calculates each of the 20 step voltages and loads them to the bias source. Since 20 steps are used for each period of the signal, the AWG Channel 1 will set the clock signal for the bias source to  $62,5 \times 20 = 1250$  Hz. Channel 2 of the AWG is adjusted to the frequency at which the digitizer will sample the signal, in

this case, 50 kHz, i.e., 800 points per period will be measured. The sampling parameters of the digitizer are set as follows: voltage range: 1 V, DCV digitizing mode, integration time: 3  $\mu$ s, and trigger mode: external. The measurement performed with these parameters over five successive periods is shown in Figure-7. There are small transition regions between the steps due to the finite transition time, where the measured voltages are not defined (zoomed-in circle). In this example, only one point is visible due to the relatively low sampling frequency, but at higher frequencies, more points will fall into the transition region. These points are discarded, and the remaining data is used to calculate the average voltages of each step and the dynamic gain of the digitizer at the given frequency.

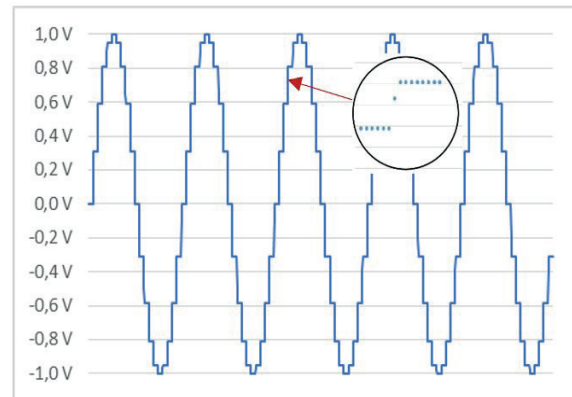


**Figure 7.** UME CPJVS Step-Approximated Sine Wave Measured by Digitizer

To determine whether the operation of the UME CPJVS in AC mode is regular, the same measurement was repeated by applying each step as a DC voltage and measuring it with the digitizer set to the same sampling parameters as for AC. The difference in voltages measured in the two different modes at each step was smaller than the standard deviation of the measurement, which proves that the system operates in a regular quantum state.

## 4. CONCLUSION

The establishment of the TÜBİTAK UME CPJVS system was presented. Full control over the system and user-friendly operation in the cryogenic cooler were the main goals of the project, and these goals were successfully achieved. The tests performed show that the system is capable of

producing a reference voltage for the calibration of DC voltage standards and can also be used in the calibration of digital converters.

## REFERENCES

- [1] Josephson B. D. *Possible new effects in superconductive tunneling*, Phys. Lett. 1962, 1 251–3
- [2] Burroughs C. J. et al., “NIST 10 V Programmable Josephson Voltage Standard System”, IEEE Transactions on Instrumentation and Measurement, vol. 60, no. 7, pp. 2482-2488, July 2011, doi: 10.1109/TIM.2010.2101191.
- [3] Lee J., Behr R., Palafox L., Schubert M., Starkloff M. and Böck A. C. *An ac quantum voltmeter based on a 10 V programmable Josephson array* Metrologia 2013, 50 612–22
- [4] Flowers-Jacobs N. E. et al, *Development and applications of a four-volt Josephson arbitrary waveform synthesizer* IEEE Int. Superconductive Electronics Conf. 2019 (ISEC 2019)
- [5] Kieler O., Behr R. and Kohlmann J. 2013a *Development of a pulse-driven AC Josephson voltage standard at PTB* ISEC 2013 Proc. 14th Int. Superconductive Electronics Conf. (Cambridge, USA) pp 59–61
- [6] Selcik S., Akyel B. and Gutmann P., “The 10V Fixed Frequency Josephson Junction Voltage Standard at UME”, CPEM 1998 Conf. Digest, p. 556 - 557, June 1998
- [7] Behr R. and Katkov A. S., “Final report on the key comparison EUROMET.BIPM.EM-K10.a: Comparison of Josephson array voltage standards by using a portable Josephson transfer standard”, Metrologia. vol. 42, Technical Supplement, 01005, 2005
- [8] Ahmadov, H. “An Oscillating Magnet Watt Balance”, 2016 Conference on Precision Electromagnetic Measurements, 09-19 July (2016), Ottawa, Canada
- [9] Arifovic M., Orhan R. and Kanatoglu N., “10 V Programmable Josephson Voltage Standard Established in TÜBITAK UME,” 2018 Conference on Precision Electromagnetic Measurements Paris, France, 2018, pp. 1-2, doi: 10.1109/CPEM.2018.8500902.
- [10] Supracon.com
- [11] Schubert M. et al, *A dry-cooled AC quantum voltmeter*, 2016 Supercond. Sci. Technol. 29 105014
- [12] Wang C, Thummes G and Heiden C *A two-stage pulse tube cooler operating below 4 K*, 1997 Cryogenics 37 159–67
- [13] Kreitman M. M. and Callahan J. T. *Thermal conductivity of apiezon N grease at liquid helium temperatures* 1970, Cryogenics 10 155–9
- [14] Hamilton C. A. et al, “A compact transportable Josephson voltage standard,” in IEEE Transactions on Instrumentation and Measurement, vol. 46, no. 2, pp. 237-241, April 1997, doi: 10.1109/19.571821.
- [15] Ünal İ., Tekbaş M., Kaya A., Coşkun Öztürk T., “Josephson Gerilim Standardı Sistemi İçin Milimetre Dalga Sentezleyici”, ELECO 2016, Bursa, Türkiye

# Why E-Commerce Startups Fail: Can machine learning provide solution?

Mona Yadegar 

Fashion design with marketing, UCSI University, Malaysia, e-mail: [mona.shokat@gmail.com](mailto:mona.shokat@gmail.com)

## Abstract

E-commerce has transformed how businesses operate, providing customers with convenience and companies with access to global markets. However, despite its vast potential, many e-commerce initiatives have failed due to either external conditions such as local or global market fluctuations or internal conditions such as a mixture of poor planning, financial mismanagement, operational inefficiencies, and cybersecurity risks. Focusing on the market fluctuations which is a key component for external conditions. A simulative dataset that mimics real-world market conditions is used to present contribution of machine learning to decision making stages. The usage of informatics could help mitigate these risks by improving decision-making, security, and operational efficiency, and in turn could prevented many of the failures.

**Keywords:** e-commerce, failure, informatics, XGBost, ML

**Citation/Atf:** YADEGAR, M. (2025). Why E-Commerce Startups Fail: Can machine learning provide solution?. *Kuantum Teknolojileri ve Enformatik Araştırmaları*. 3(1): e2753, DOI: 10.70447/ktve.2753

**Corresponding Author/ Sorumlu Yazar:**  
Mona Yadegar  
E-mail: [mona.shokat@gmail.com](mailto:mona.shokat@gmail.com)



Bu çalışma, Creative Commons Atıf 4.0 Uluslararası Lisansı ile lisanslanmıştır.  
This work is licensed under a Creative Commons Attribution 4.0 International License.

## INTRODUCTION

E-commerce heavily relies on accessibility, speed in delivery, and sharing and exchanging goods, services and information on demand [1], [2], [3]. The rise of e-commerce has been fueled by advances in technology, growing internet accessibility, and changing consumer habits [4] [5]. While some businesses thrive in this digital landscape, many others struggle to survive [6], [7]. Researches suggests that a significant percentage of e-commerce startups fail within their first few years [8]. Understanding why these failures occur is essential for businesses looking to create sustainable and successful online ventures.

The collapse of companies like Webvan, Boo.com, Etoys, Flooz.com and Quibi highlights the consequences of poor planning and execution [9], [10]. Among them, Webvan was founded in 1996, with \$1.2 billion funding, a startup that aimed to transform the grocery industry by offering online ordering and home delivery. Unfortunately, neglecting crucial factors such as not having a viable business model, avoiding sustainable cost management, and comply with market dynamics contributed to the failure in 2001 [11], [12]. Similarly, Boo.com was a promising online fashion retailer, launched in 1999. A cutting-edge online shopping experience for high-end consumers was in the plan. Unrealistic spending and unclear direction gradually steered to its failure in 2000 [13], [14].

Multiple studies present post-mortem analysis about the reasons of failure [10], [15]. Some of the emerging common threads can be outlines as follows; an inability to generate sustainable revenue due to ignoring the market dynamics, bad product-market fit due to not conducting any market research, losing to competitors as a result of lacking market oriented management, and simply running out of money because of unnecessary or misguided expansion or expenditure.

Through the manuscript, the cause of failure split into two main groups; external conditions such as local or global market fluctuations etc. and internal conditions such as a mixture of poor

planning, financial mismanagement, operational inefficiencies, and cybersecurity risks etc. These are groups usually includes country-specific conditions and can be expanded without any restriction.

The initial aim of this manuscript is to outline internal conditions from the literature review. The second aim is to demonstrate how the inability to utilize informatics and data-driven decision-making can result in business failure and then use of Machine learning (ML) to help overcome some of these challenges.

A condense literature review presented in the following sections. Key Reasons for E-Commerce Failure are abstracted from references given in the text. Then, a microdata set that is artificially generated that mimics market conditions is used to present contribution of ML to decision making stage. Some suggestions are outlined for future e-commerce attempts.

### **The Role of Informatics in E-Commerce**

In the context of this study, the term, informatics refers to the collection large volume of the data, processing them for multi-purpose, and application of the findings to elevate business via using in decision-making and also operations [16], [17], [18]. In simple terms, informatics helps e-commerce companies to analyze consumer behavior, optimize inventory, enhance cybersecurity, and personalize marketing strategy [19].

One of the most impactful applications of informatics is in big data analytics [20]. At this stage ML applications come into use, as it happens in different scientific applications [21], [22], [23], [24]. ML and big data can evaluate customer preferences and predict tendency of buying in future, and then modify inventory requests accordingly. As a result, the usage of the informatics helps companies to avoid both stock shortages of highly demanded products and also overstocking low demanded goods.

Addition to managing the market, cybersecurity is another vital area where informatics comes into play [25], [26]. Advanced encryption, artificial intelligent (AI) driven fraud detection [27], and

blockchain technology [28] help protect sensitive customer information from cyber threats which also uses similar technology [29].

Note that informatics enables seamless integration of different e-commerce functions, such as payment processing, customer relationship management, and supply chain tracking [30], [31]. By automating and optimizing these processes, both conventional and online businesses can reduce operational costs and improve efficiency.

### Key Reasons for E-Commerce Failure

A quote attributed to Benjamin Franklin states that. "If You Fail to Plan, You Are Planning to Fail". It is still valid axiom. Regardless of being conventional or e-commerce initiative all commercial activities require careful planning ahead. This actions requires knowledge. Lack of knowledge or misinterpretation of the data drags the company to unwanted locations. The following compilations from literature summarizes some of the reasons for failure. Note that this list is not exhausted list and can be extend beyond the limit of the manuscript.

A) Pre- launching period;

**Inadequate Market Research**, many e-commerce ventures fail because they don't understand their audience or industry well enough. Entrepreneurs sometimes launch platforms without fully grasping market demand, consumer behavior, or competitive landscapes [32]. Without this critical knowledge, businesses often invest resources in the wrong places and struggle to attract customers.

**Poor User Experience (UX) and Website Design**, customers expect a seamless and intuitive online shopping experience. Issues such as slow loading times, confusing navigation, and a lack of mobile optimization can frustrate users and lead to high bounce rates and abandoned carts [33]. A lack of personalization and poor customer support further deter potential buyers.

B) Operational period

**Security and Privacy Concerns**, consumers need to trust an e-commerce platform before making

a purchase. Security breaches, weak encryption, and unprotected payment gateways expose businesses and customers to fraud [34]. Failing to implement strong security measures can result in financial losses and a damaged reputation.

**Logistical and Supply Chain Challenges**, timely and reliable order fulfillment is a crucial part of e-commerce success. Businesses that struggle with inventory management, shipping delays, or inefficient return policies risk losing customer trust [35]. Without streamlined logistics, even the best products can fail to reach the right customers at the right time.

C) Management issues

**Financial Mismanagement**, many startups overestimate their potential revenue while underestimating operational costs [36]. Poor budgeting, unsustainable pricing models, and cash flow problems can quickly sink a business. Without a solid financial plan, even promising e-commerce ventures can run out of resources before they gain traction.

**Ineffective Digital Marketing Strategies**, in a highly competitive online space, businesses need strong digital marketing strategies to attract and retain customers. A lack of SEO optimization, weak social media presence, and poorly targeted advertisements result in low visibility and poor sales [37]. Simply having a website is not enough, businesses must actively engage their audience.

D) Site-depended problem

**Regulatory and Compliance Issues**, ignoring legal and regulatory requirements of where seller or buyer are located, such as tax laws, consumer protection rules, and data privacy policies, can lead to serious consequences [38]. Businesses that fail to comply with these regulations risk lawsuits, fines, and even shutdowns.

Figure 1 illustrate the relation between key reasons and failure. Similar to conventional usage of Venn diagram which usually address the recipe for success, the startups are expected to cover red zone to survive.

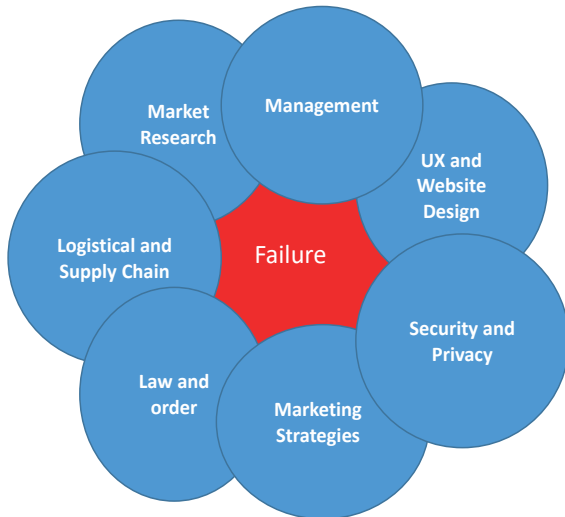


**Figure 1.** Simplified relation between key reasons and failure. The smaller the red zone, the higher the probability of the company's survival

The area of red zone in Figure 1 should be next to none to increase the survival rate. This can be achieved via improving either or multiple keys. Aforementioned issues are the recipes to doom even once-successful companies. Integrating informatics into e-commerce operations can help businesses prevent many of the common pitfalls that lead to failure. Data-driven decision-making allows businesses to anticipate market trends, streamline logistics, and adjust strategies in real time.

**Data driven decision maker**

The external conditions are usually seen as out-of-control situations but also accepted that the occurrence can be predicted up to certain level [39]. Traditionally, over simplified approach uses stock market data to guide the investment decision. Two periods outlines the approach; Bull and Bear cycles (Figure 2). A bull market refers to a period of rising stock prices. It is assumed that increasing investor confidence, strong economic growth, and low unemployment rates occur in this period. On the other hand, a bear market is about the declining stock prices, economic contraction, and reduced investor confidence. Hence, it represent macroeconomic downturns, high inflation, or financial crises [40].

Numerically, the threshold is about 20% or more change from their previous period [41]. Bull markets represent the upward change, while bear markets shows a decline [42].

Strategic decisions should be in accord with these cycles. Bull markets states that companies may expand their investment in research and development, acquire competitors, and upscale their operations. While bear markets are the periods when firms are forced to cut costs, to preserve liquidity, and downsize their operations so that they can survive through economic



**Figure 2.** Variations and market definitions [43].

declines [44], [45].

Regardless of the size of the company, relying on single data is not viable. Multiple criteria, such as stock returns, inflation rates, interest rates, etc., must always be employed for holistic approach [46].

A simplified ML application can be explain through a scenario. Note that this neither final recommendation not optimum solution, It is just an example using financial indicators to predict optimal investment time, i.e., Bull cycle. According to result, the decision makers may take action to expand or shrink a business.

**Scenario:** using a data set covering over approximately 15 years, can we guide the investment strategy in March 2025?

The solution requires internal i.e., key performance indicators (KPIs) and external data i.e., major indicators of economic conditions. Ahmed et al [47] states that the success of an e-commerce company can be measured using KPIs across different areas, including financial health, customer engagement, and operational efficiency. In the frame of this study only financial performance and customer acquisition were taken into consideration. Marketing performance and operational efficiency and many other possible indicators were left out for the sake of the simplicity.

Selected financial performance indicators are as follows. Revenue growth which represent variations in sales over the time. Profit margins measures the health of profitability. Average Order Value (AOV) means spending per purchase. Customer Lifetime Value (CLV) is a measurement of the loyalty of customer and repeatability of business.

Indicators for customer acquisition & retention will be defined under the three basic definitions. Customer acquisition cost (CAC) together with CLV measures the sustainability of business. Repeat purchase rate indicates strong brand loyalty. Conversion rate is the percentage of visitors who make a purchase.

For this purposes I generated a random dataset

that mimics real-world market conditions via simulating selected KPIs and also stock returns together with changes in both inflation rates and interest rates. Needless to say that the business owners can use real data according to country of origin and also increase the number of criteria in accordance with the availability of data.

To make this decision, the proposed algorithm (Figure 3) uses *XGBoost*, a widely recognized gradient boosting algorithm known for its efficiency in financial time-series predictions [48]. A simple code was developed in Python, with the help of AI applications, is given in Amendment.

In general, XGBoost uses gradient boosting tree mode, the model follows an additive approach, combining multiple decision trees:

$$\tilde{y} = \sum_i^N f_i(X) \quad (1)$$

Where X type of the data available, N number of trees  $f_i(X)$  the prediction of the i-th tree, and finally  $\tilde{y}$ , predicted values of y. The development and evaluation of Equation 1 can be found literature and web pages and will not be repeated here (please see [48], [49]). For clarity, X contains KPIs, stock returns, and changes in both inflation rates and interest rates in this scenario while y-values are 0 or 1 along the coverage period (15 years). y-values controls the success of the approach and should be selected with caution. Murphy [48] suggested that stock market trends can be used to predict possible investment time.

If the 50-day simple moving average (SMA) crosses above the 200-day SMA (y=1), it often signals a good time to invest. Otherwise, it is time to act conservatively and wait (y=0). Figure 4 shows real stock market data obtained from yahoo finance. Comparison of SMA\_50 and SMA\_200 suggests that 2024 presents a favorable opportunity for business expansion, particularly if the interest rates are low, provided that key performance indicators remain aligned.

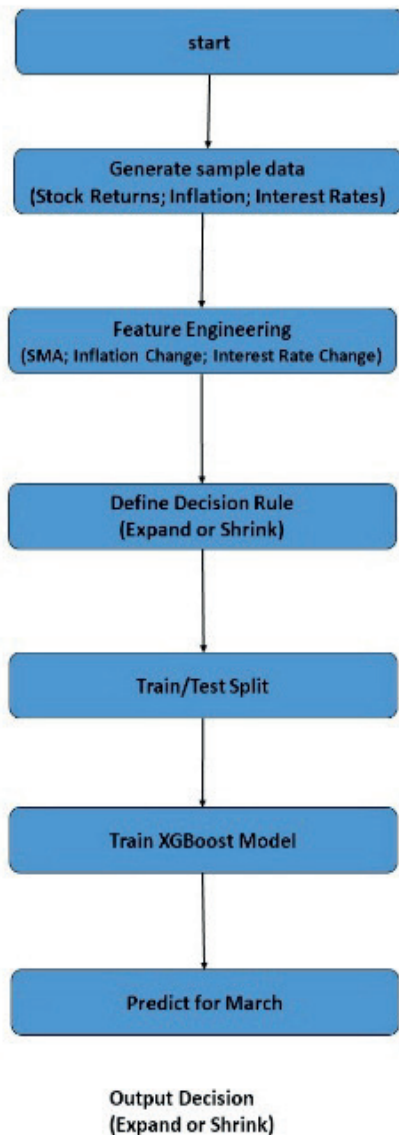


**Figure 3.** algorithm of the decision making

The algorithm trained the model using 80% of the data set and then the rest of the data were used to test for accuracy. The model learned to predict whether market conditions suggest favorable expansion time ( $\tilde{y} = 1$ ) or staying steady or shrinking time ( $\tilde{y} = 0$ ). This approach aligns with prior research on economic cycle forecasting [50]. As a next stage, the trained model evaluates data and determine whether economic conditions in expected time (e.g. March 2025) favor business expansion or contraction. The result was positive ( $\tilde{y} = 1$ ) for this scenario but irrelevant since it was based on random data set. Real-life example should include company-specific KPI and external data for meaningful result.

This approach would allow for a robust dynamic, data-driven, decision-making process rather than relying solely on intuition or traditional analysis.

## DISCUSSION

The result of the ML applications are heavily rely on the data. The consistency of the data set controls the output. Figure 5 shows the actual ( $y$ ) and predicted ( $\tilde{y}$ ) decision over Last 100 Days.

There was one incidence that result was false i.e., actual decision is 0 but predicted is 1. Number of tests with various random data set pointed out that any unusual fluctuation in stock market could easily cause such false result. Thus, multiple decision criteria should be tested before taking any action. In addition to guiding investment strategy, ML can be used for management purposes and enhances operational efficiency. Automated inventory management, real-time order tracking, and AI-powered pricing adjustments help businesses stay competitive [51]. By reducing human errors and improving response times, e-commerce companies can improve both their internal processes and customer satisfaction [52].

As an example, considering the predictive analytics, and through the examination of historical sales data, companies are able to make decisions regarding inventory management, thereby ensuring that they maintain appropriate stock levels of the correct products [53]. This approach mitigates the potential for lost sales resulting from stock shortages or the necessity to offer significant discounts on surplus inventory.

Security threats are another major concern for e-commerce businesses. Informatics-driven security systems, such as AI-powered fraud detection and multi-factor authentication, help protect against cyberattacks and fraudulent transactions [54]. These technologies help businesses maintain customer trust and prevent financial losses.

Customer experience is also greatly enhanced by informatics. Personalized recommendations, automated chatbots, and AI-driven customer support improve engagement and satisfaction



Figure 4. Comparison of SMA\_50 and SMA\_200 for stock market data obtained from Yahoo finance web site.

[55]. Businesses that understand and anticipate their customers' needs are more likely to build long-term relationships and foster brand loyalty. Informatics-driven e-commerce has transformed the retail landscape, offering numerous benefits such as increased efficiency and personalized shopping experiences. However, it also presents several challenges [56], [57], [58], [59].

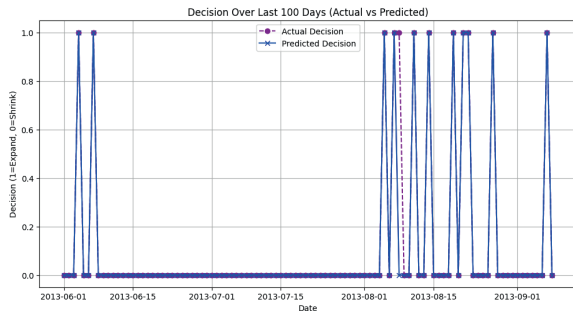


Figure 5. Comparison of decisions; actual ( $y$ ) with solid line and predicted ( $\hat{y}$ ) with dashed line

Establishing and maintaining advanced e-commerce systems require significant investments in infrastructure, software, and cybersecurity measures, contributing to increased operational expenses. Technical glitches, server crashes, or software bugs can lead to operational disruptions. Providing accessibility around the clock and along the year is a major concern to keep e-business in business [60].

While automation enhances efficiency, excessive dependence on AI-driven customer service may lack the personal touch, potentially leading to customer frustration. Talking to Chabot is not pleasant experience especially non-native speakers and elderlyes. In addition, AI algorithms in e-commerce can unintentionally perpetuate biases present in their training data, leading to discriminatory practices or unfair pricing strategies.

As stated above, e-commerce businesses must navigate complex regulations related to data protection, taxation, consumer rights and environmental regulations. As an example, the rise of e-commerce has led to increased packaging waste and carbon emissions from shipping, raising concerns about its environmental sustainability.

A simple real-life example can simulate the some of the major issues mentioned above. If an entrepreneur starting a business in the Middle East to sell her art globally, even within her own country. A product will cost only \$20, but a 25% tax must be added for the government and then an average 18% fee for the e-commerce platform will elevate the price. In addition, the cost of the cargo fee makes the final cost undesirable and ultimately leads the entrepreneur towards failure.

Alternatively, considering the same entrepreneur is trying an international platform to reach the global market, where there are no visible taxes involved. However, the shipping costs are three times higher than the product itself and the high custom fee depending on the country of arrival will cost fortune to buyer. After all, additional taxing for transferring of the money to country of the origin will make the commercial attempt sink into dark hole of failure.

It is worth to mention that the security breach is another problem for e-commerce businesses. The extensive collection of personal data in e-commerce platforms makes their database prime targets for cyberattacks, leading to potential financial losses for both parties. Nalla and Reddy [61] compared modern and conventional database solutions and stated that a security breach rates are 15% and 25% respectively.

As a summary, regular problems related to conventional business operation require management skill which can be enhanced via analyzing the data and utilizing knowledge.

E-commerce challenges outlined above underscored the importance of implementing robust security measures, ethical AI practices, and inclusive strategies to mitigate the all impacts of informatics-driven e-commerce.

## RESULTS

The E-Commerce Performance Model provides a systematic framework for analyzing the reasons behind the failure of e-commerce businesses by evaluating KPIs [62], [63]. Table 1 summaries the some of the common indicators that may lead to an undesired point. These indicators can be extend according to industry, local law and regulations and geographic location.

By leveraging data analytics and performance models, e-commerce businesses can diagnose failures in advance, optimize processes accordingly, and implement corrective measures to enhance overall performance [64].

Through the manuscript only one numerical example was presented in order to fit the frame of the publication. With the selection of appropriate data set and decision criteria, the code presented here can be altered to serve to predict future of any KPIs.

## CONCLUSION

The e-commerce businesses keep failing due to skipping or doing poorly market research, not responding and heal the bad user experiences on time, being open to security breaches, logistical inefficiencies, and most important overlooking the market dynamics and financial mismanagement.

**Table 1.** Some of the indicators to foresee the future

Indicators	Sustainable	Unsustainable
Marketing strategies	$CAC < CLV$	$CAC > CLV$
Long-Term Investment	Data-driven	Intuitive
Conversion rates	High	Low
Operational efficiency	Fast	Slow
Return rates	Low	High
Inventory Turnover*	High	Low
Cost saving	High	low
Supply Chain	High percentage of suppliers	Struggling to find suppliers
Digital Transformation	In pace with development	Only basic usage

\*The optimum turnover ratio varies by industry. High-Turnover Industries focuses on regular products aiming for daily needs. Low-Turnover Industries are for the niche products such as luxury goods, heavy machinery, and specialty items.

However, many of these failures can be mitigated with the right application of informatics and usage of the data-driven actions providing that the data the decision are appropriate and consistent.

Informatics frameworks, particularly Big Data Analytics and AI-driven market prediction, provide robust tools for market forecasting and business decision-making. By leveraging data analytics, enhancing cybersecurity, optimizing operations, and improving customer engagement, businesses can avoid common pitfalls and increase their chances of long-term success.

In harsh competitive environment, e-commerce companies must not only embrace informatics but also integrate it into every aspect of their strategy and operations to thrive in the digital age.

### Acknowledge

The author would like to thank the anonymous referees for improving the clarity of the manuscript.

### REFERENCES

- [1] P. Barnes-Vieyra and C. Claycomb, "Business-to-Business E-Commerce: Models and Managerial Decisions," *Bus. Horiz.*, vol. 44, no. 3, pp. 13–13, May 2001.
- [2] R. Javalgi and R. Ramsey, "Strategic issues of e-commerce as an alternative global distribution system," *Int. Mark. Rev.*, vol. 18, no. 4, pp. 376–391, Aug. 2001, doi: 10.1108/02651330110398387.
- [3] G. C. Ariguzo, E. G. Mallach, and D. S. White, "The first decade of e-commerce," *Int. J. Bus. Inf. Syst.*, Jan. 2006, Accessed: Apr. 03, 2025. [Online]. Available: <https://www.inderscienceonline.com/doi/10.1504/IJBIS.2006.008598>
- [4] M. J. Epstein, "Implementing successful e-commerce initiatives," *Strateg. Finance*, vol. 86, no. 9, p. 22, 2005.
- [5] B. S. Vijayaraman and G. Bhatia, "A Framework for Determining Success Factors of an E-Commerce Initiative," *J. Internet Commer.*, Mar. 2002, doi: 10.1300/J179v01n02\_05.
- [6] L. Murillo, "Supply chain management and the international dissemination of e-commerce," *Ind. Manag. Amp Data Syst.*, vol. 101, no. 7, pp. 370–377, Oct. 2001, doi: 10.1108/EUM000000005825.
- [7] J. Rovenpor, "Explaining the E-Commerce Shakeout: Why Did So Many Internet-Based Businesses Fail?," *E-Serv. J.*, vol. 3, no. 1, pp. 53–76, 2003, doi: 10.1353/esj.2004.0011.
- [8] K. C. Laudon and C. G. Traver, *E-commerce: Business, Technology, Society: Global Edition*. 2021. [Online]. Available: <https://www.pearson.com/en-us/subject-catalog/p/e-commerce-2021-business-technology-and-society/P200000001390/9780136931829>
- [9] "5 failed startups that defined an era," *FasterCapital*. [Online]. Available: <https://fastercapital.com/topics/5-failed-startups-that-defined-an-era.html>
- [10] N. Bahra, "How to Avoid Failure," in *Competitive Knowledge Management*, Palgrave Macmillan, London, 2001, pp. 139–150. doi: 10.1057/9780230554610\_10.
- [11] W. Aspray, G. Royer, and M. G. Ocepek, "Anatomy of a dot-com failure: the case of online grocer Webvan," in *Food in the Internet Age*, 2013. Accessed: Apr. 03, 2025. [Online]. Available: <https://link.springer.com/book/10.1007/978-3-319-01598-9>
- [12] C. Galea and S. Walton, "Is E-Commerce Sustainable?: Lessons from Webvan," in *The Ecology of the New Economy*, Routledge, 2017, pp. 100–109. doi: 10.4324/9781351282048-8.
- [13] G. J. Stockport, G. Kunnath, and R. Sedick, "Boo.com—The path to failure," *J. Interact. Mark.*, Nov. 2001, doi: 10.1002/dir.1023.
- [14] I. Chaston, *An Entrepreneurial Disaster -Boo.com*. SAGE Publications Ltd, 2009. doi: 10.4135/9781473939059.
- [15] M. A. Razi and J. M. Tarn, "Exploring dotcom failure: A mediator modeling approach," *Hum. Syst. Manag.*, Dec. 2004, Accessed: Apr. 04, 2025. [Online]. Available: <https://journals.sagepub.com/doi/abs/10.3233/HSM-2004-23407>
- [16] Aslan, M, "Management Information Systems and Strategic Decision-Making," in *Mert, G., Şen, E., Yılmaz, O.(Editörler), Data, Information and Knowledge Management*, 2020.
- [17] L. Nikiforova, "Use of innovative information technology in e-commerce and digital economy,"

- Innov. Sustain.*, 2022, doi: 10.31649/ins.2022.1.65.71.
- [18] O. Cherednichenko, O. Ivashchenko, M. Lincényi, and M. Kováč, "Information technology for intellectual analysis of item descriptions in e-commerce," *Entrep. Sustain. Issues*, vol. 11, no. 1, pp. 178–190, 2023, doi: 10.9770/jesi.2023.11.1(10).
- [19] M. F. Rabbi, M. B. Amin, M. Al-Dalahmeh, and M. Abdullah, "Assessing the role of information technology in promoting environmental sustainability and preventing crime in E-commerce," Aug. 2024, doi: 10.1556/1848.2024.00834.
- [20] J. Zakir, T. Seymour, and K. Berg, "Big data analytics," *Issues Inf. Syst.*, vol. 16, no. 2, pp. 81–90, 2015, doi: 10.48009/2\_iis\_2015\_81-90.
- [21] E. Alpaydın, *Machine Learning*. The MIT Press, 2016. Accessed: Apr. 03, 2025. [Online]. Available: <https://mitpress.mit.edu/9780262529518/machine-learning/>
- [22] B. Köse, "Veri, Enformatik, Yapay Zeka ve Optimizasyon," *J. Quantum Technol. Inform. Res.*, vol. 1, no. 1, Art. no. 1, Oct. 2023, doi: 10.70447/ktve.2241.
- [23] A. Erçel and E. U. Uluggerli, "Öğrenen Makineler Ve Fasiyes Ayrımı; İlk Sonuçlar: *J. Quantum Technol. Inform. Res.*, vol. 2, no. 1, Art. no. 1, Feb. 2024, doi: 10.70447/ktve.2322.
- [24] D. Çokay and E. Şahi, "Makine Öğrenme Algoritmaları Kullanarak Ses Verilerinde Hastalık Tespiti," *J. Quantum Technol. Inform. Res.*, vol. 2, no. 2, Art. no. 2, 2024, doi: 10.70447/ktve.2422.
- [25] D. C. Rowe, B. M. Lunt, and J. J. Ekstrom, "The role of cyber-security in information technology education," in *Proceedings of the 2011 conference on Information technology education*, 2011. doi: 10.1145/2047594.204762.
- [26] I. H. Sarker, A. S. M. Kayes, S. Badsha, H. Alqahtani, P. Watters, and A. Ng, "Cybersecurity data science: an overview from machine learning perspective," *J. Big Data*, vol. 7, no. 1, Art. no. 1, Dec. 2020, doi: 10.1186/s40537-020-00318-5.
- [27] M. S. Islam and N. Rahman, "AI-Driven Fraud Detections in Financial Institutions: A Comprehensive Study," *J. Comput. Sci. Technol. Stud.*, vol. 7, no. 1, Art. no. 1, Jan. 2025, doi: 10.32996/jcsts.2025.7.1.8.
- [28] M. Abdelhamid, L. Sliman, R. Djemaa, and G. Perboli, "A Review on Blockchain Technology, Current Challenges, and AI-Driven Solutions," *ACM Comput. Surv.*, Nov. 2024, doi: 10.1145/3700641.
- [29] B. Guembe, A. Azeta, S. Misra, V. C. Osamor, L. Fernandez-Sanz, and V. Pospelova, "The Emerging Threat of Ai-driven Cyber Attacks: A Review," *Appl. Artif. Intell.*, Dec. 2022, Accessed: Apr. 03, 2025. [Online]. Available: <https://www.tandfonline.com/doi/abs/10.1080/08839514.2022.2037254>
- [30] D. Hindarto, "The Role of E-Commerce in Increasing Sales Using Unified Modeling Language," *Int. J. Softw. Eng. Comput. Sci. IJSECS*, vol. 3, no. 2, Art. no. 2, Aug. 2023, doi: 10.35870/ijsecs.v3i2.1503.
- [31] G. C. Oguta, "Securing the virtual marketplace: Navigating the landscape of security and privacy challenges in E-Commerce," *GSC Adv. Res. Rev.*, vol. 18, no. 1, Art. no. 1, 2024, doi: 10.30574/gscarr.2024.18.1.0488.
- [32] D. Chaffey, *Digital business and e-commerce management : strategy, implementation and practice*. Pearson, 2015. Accessed: Apr. 03, 2025. [Online]. Available: <https://thuvienso.hoasen.edu.vn/handle/123456789/8548>
- [33] J. Nielsen, *Designing Web Usability: The Practice of Simplicity*. 1999. doi: 10.5555/519216.
- [34] G. P. Schneider, *Electronic commerce*. Cengage Learning, 2015. Accessed: Apr. 04, 2025. [Online]. Available: <https://thuvienso.hoasen.edu.vn/handle/123456789/8021>
- [35] P. Kotler, K. L. Keller, and A. Chernev, *Marketing management*, 16th ed. Pearson, 2022. [Online]. Available: <https://www.pearson.com/en-us/subject-catalog/p/marketing-management/P200000005952/9780137344161>
- [36] E. Turban, C. Pollard, and G. Wood, *Information technology for management: Advancing sustainable, profitable business growth*, 12th ed. Wiley, 2020.
- [37] D. Ryan, *Digital marketing: Strategy, implementation, and practice*, 7th ed. Pearson, 2021.
- [38] A. Kwilinski, R. Volynets, I. Berdnik, M. Holovko, and P. Berzin, "E-Commerce: Concept and legal regulation in modern economic conditions," *J. Leg. Ethical Regul. Issues*, vol. 22, no. 2, 2019, [Online]. Available: <https://heionline.org/HOL/LandingPage?handle=hein.journals/jnlolletl22>
- [39] R. A. De Santis and W. Van der Veken, "Forecasting macroeconomic risk in real time: Great and Covid-19 recessions," ECB Working Paper, Working Paper 2436, 2020. doi: 10.2866/019813.
- [40] R. J. Shiller, *Irrational Exuberance*, 3rd ed.

- Princeton University Press, 2015. Accessed: Apr. 04, 2025. [Online]. Available: <https://www.torrossa.com/en/resources/an/5559001>
- [41] A. R. Pagan and K. A. Sossounov, "A simple framework for analysing bull and bear markets," 2003, doi: 10.1002/jae.664.
- [42] B. G. Malkiel, *A random walk down Wall Street: The time-tested strategy for successful investing*, 12th ed. New York, London: W. W. Norton & Company, 2019.
- [43] J. Lawler, "Bull market vs Bear market: Everything you need to know," capital.com. Accessed: Apr. 04, 2025. [Online]. Available: <https://capital.com/bull-market-vs-bear-market>
- [44] P. L. Bernstein and R. D. Arnott, "Bull market? Bear market?, Should you really care?," *J. Portf. Manag.*, vol. 24, no. 1, p. 26, 2006.
- [45] Damodaran, A., *Investment Valuation*. Wiley, 2012. Accessed: Apr. 03, 2025. [Online]. Available: [https://books.google.com/books/about/Investment\\_Valuation.html?hl=tr&id=cjwGfjHGkC](https://books.google.com/books/about/Investment_Valuation.html?hl=tr&id=cjwGfjHGkC)
- [46] A. F. Burns and W. C. Mitchell, "Measuring Business Cycles," National Bureau of Economic Research, burn46-1, Jan. 1946. Accessed: Apr. 03, 2025. [Online]. Available: <https://www.nber.org/books-and-chapters/measuring-business-cycles>
- [47] H. Ahmed, T. A. Jilani, W. Haider, M. A. Abbasi, S. Nand, and S. Kamran, "Establishing Standard Rules for Choosing Best KPIs for an E-Commerce Business based on Google Analytics and Machine Learning Technique," *Int. J. Adv. Comput. Sci. Appl. Ijacs*, vol. 8, no. 5, Art. no. 5, Nov. 2017, doi: 10.14569/IJACSA.2017.080570.
- [48] T. Chen and C. Guestrin, "XGBoost: A Scalable Tree Boosting System," in *ACM Conferences*, 2016. doi: 10.1145/2939672.293978.
- [49] C. Bentéjac, A. Csörgő, and G. Martínez-Muñoz, "A comparative analysis of gradient boosting algorithms," *Artif. Intell. Rev.*, vol. 54, no. 3, pp. 1937–1967, Mar. 2021, doi: 10.1007/s10462-020-09896-5.
- [50] J. H. Stock and W. M. Watson, "Forecasting Output and Inflation: The Role of Asset Prices," *J. Econ. Lit.*, vol. 41, no. 3, pp. 788–829, Sep. 2003, doi: 10.1257/002205103322436197.
- [51] M. Awais, "Optimizing Dynamic Pricing through AI-Powered Real-Time Analytics: The Influence of Customer Behavior and Market Competition," *Qlantia J. Soc. Sci.*, vol. 5, no. 3, Art. no. 3, Sep. 2024, doi: 10.55737/qjss.370771519.
- [52] M. S. Bhuiyan, "The Role of AI-Enhanced Personalization in Customer Experiences," *J. Comput. Sci. Technol. Stud.*, vol. 6, no. 1, Art. no. 1, Feb. 2024, doi: 10.32996/jcsts.2024.6.1.17.
- [53] F. Jack and R. Bommu, "Unveiling the Potential: AI-Powered Dynamic Inventory Management in the USA," *Int. J. Adv. Eng. Technol. Innov.*, vol. 3, no. 1, Art. no. 1, Jul. 2024.
- [54] A. Mudgal, "Leveraging AI and ML for Proactive Threat Detection for E-Commerce," in *Strategic Innovations of AI and ML for E-Commerce Data Security*, IGI Global Scientific Publishing, 2025, pp. 281–322. doi: 10.4018/979-8-3693-5718-7.ch012.
- [55] B. Singh and C. Kaunert, "AI-Driven Strategies for Customer Engagement, Market Segmentation, and Resource Optimization: Projecting End User Satisfaction and Futuristic Growth of Business," in *AI Innovations in Service and Tourism Marketing*, IGI Global Scientific Publishing, 2024, pp. 104–128. doi: 10.4018/979-8-3693-7909-7.ch006.
- [56] T. M. Le and S.-Y. Liaw, "Effects of Pros and Cons of Applying Big Data Analytics to Consumers' Responses in an E-Commerce Context," *Sustainability*, vol. 9, no. 5, Art. no. 5, May 2017, doi: 10.3390/su9050798.
- [57] R. LaRose, "On the Negative Effects of E-Commerce: a Sociocognitive Exploration of Unregulated on-line Buying," 2001, Accessed: Apr. 04, 2025. [Online]. Available: <https://dx.doi.org/10.1111/j.1083-6101.2001.tb00120.x>
- [58] F. Ho, "The Dark Side of E-Commerce: The Negative Effects of E-Commerce on the Environment," *Brooklyn J. Corp. Financ. Commer. Law*, 2022, Accessed: Apr. 03, 2025. [Online]. Available: <https://home.heinonline.org/>
- [59] M. Soleimani, "Buyers' trust and mistrust in e-commerce platforms: a synthesizing literature review," *Inf. Syst. E-Bus. Manag.*, vol. 20, no. 1, pp. 57–78, Mar. 2022, doi: 10.1007/s10257-021-00545-0.
- [60] N. Bajgoric, "Keeping e-business in business: identifying the new perspective of server operating systems," *Int. J. Bus. Inf. Syst.*, Jun. 2017, Accessed: Apr. 03, 2025. [Online]. Available: <https://www.inderscienceonline.com/doi/10.1504/IJBIS.2017.084433>
- [61] L. N. Nalla and V. Reddy M., "Data Privacy and Security in E-commerce: Modern Database Solutions," *Int. J. Adv. Eng. Technol. Innov.*, vol. 1, no. 3, pp. 248–263, 2023.
- [62] S. Krishnamurthy, *E-Commerce Management*.

2002. doi: 10.5555/515304.

- [63] K. C. Laudon and C. G. Traver, *E-commerce 2023: Business, technology, society*. Pearson, 2023. [Online]. Available: <https://www.pearson.com/en-us/subject-catalog/p/e-commerce-2023-business-technology-society/P200000009801/9780138043391>
- [64] T. H. Davenport and J. G. Harris, "Competing on analytics: The new science of winning," *Harv. Bus. Rev. Press*, 2017, [Online]. Available: <https://hbr.org/2006/01/competing-on-analytics>

## Amendment

```
import pandas as pd
import numpy as np
import xgboost as xgb
from sklearn.model_selection import train_test_split
import matplotlib.pyplot as plt

# Sample data - Replace with real data
# Define the data set
np.random.seed(42)
date_range = pd.date_range(start="2000-01-01",
periods=5000, freq='D')
data = pd.DataFrame(index=date_range)

# Financial Performance Indicators
data['Revenue_Growth'] = np.random.uniform(0.95,
1.05, size=len(date_range))
data['Profit_Margin'] = np.random.uniform(5, 30,
size=len(date_range))
data['AOV'] = np.random.uniform(50, 500,
size=len(date_range))
```

```
data['CLV'] = np.random.uniform(100, 2000,
size=len(date_range))

# Customer Acquisition & Retention
data['CAC'] = np.random.uniform(5, 50,
size=len(date_range))
data['Repeat_Purchase_Rate'] =
np.random.uniform(0.1, 0.5, size=len(date_range))
data['Conversion_Rate'] = np.random.uniform(0.01,
0.2, size=len(date_range))

# Generate a linear trend with breaks represent bears
and bulls
def linear_trend_with_breaks(length, breaks, slopes):
    trend = np.zeros(length)
    start = 0
    for i, (break_point, slope) in enumerate(zip(breaks,
slopes)):
        end = break_point if i < len(breaks) - 1 else
length
        trend[start:end] = np.arange(0, end - start) *
slope + trend[start - 1] if start > 0 else np.arange(0,
end - start) * slope
        start = end
    return trend

breaks = [1250, 2000, 2500, 2700, 3750] # Define
the break points
slopes = [0.01, -0.05, 0.01, -0.1, 0.02] # Define the
slopes for each segment, negative values means
downturns
data['Linear_Trend'] =
linear_trend_with_breaks(len(date_range), breaks,
slopes)

# Add random noise to the linear trend to create the
'Return' column
data['Return'] = data['Linear_Trend'] +
np.random.normal(-50, 50, size=len(date_range))
+100 # Random noise added

# External indicators
data['Inflation'] = np.random.uniform(1.5, 3.5,
size=len(date_range))
```

```

data['InterestRate'] = np.random.uniform(0.5, 5.0,
size=len(date_range))
data['Inflation_Change'] =
data['Inflation'].pct_change().fillna(0)
data['InterestRate_Change'] =
data['InterestRate'].pct_change().fillna(0)
# End data definition to be replace with real data

# Decision Criteria
data['SMA_50'] =
data['Return'].rolling(window=50).mean().fillna(0)
data['SMA_200'] =
data['Return'].rolling(window=200).mean().fillna(0)
data['Decision'] = np.where(
    (data['SMA_50'] > data['SMA_200']) &
    (data['InterestRate'] < 2.5) &
    (data['Conversion_Rate'] > 0.05), 1, 0
)

# Train/Test Split
features = ['Return', 'SMA_50', 'SMA_200',
'Inflation_Change', 'InterestRate_Change',
'Revenue_Growth', 'Profit_Margin', 'AOV',
'CLV', 'CAC', 'Repeat_Purchase_Rate',
'Conversion_Rate']
X = data[features]
y = data['Decision']
X_train, X_test, y_train, y_test = train_test_split(X,
y, test_size=0.2, random_state=42)

# Train XGBoost Model
model =
xgb.XGBClassifier(use_label_encoder=False,
eval_metric='logloss')
model.fit(X_train, y_train)

# Plot SMA_50 and SMA_200
plt.figure(figsize=(12, 6))
plt.plot(data.index, data['SMA_50'], label='SMA_50')
plt.plot(data.index, data['SMA_200'],
label='SMA_200')
plt.title('SMA_50 vs SMA_200')
plt.xlabel('Date')
plt.ylabel('Value')
plt.legend()

```

```

plt.grid(True)
plt.show()

# Select the Prediction month (March=3)
march_data = data.loc[data.index.month == 3,
X.columns]
prediction = model.predict(march_data)
result = "Expand" if prediction[-1] == 1 else "Shrink"
print(f'Decision for March: {result}')

# Plot Decision Over Last 100 Values with Model
Prediction
plt.figure(figsize=(12, 6))
plt.plot(data.index[-100:], data['Decision'][-100:],
label='Actual Decision', color='purple', linestyle='--',
marker='o')
predicted_decisions = model.predict(X.iloc[-100:])
plt.plot(data.index[-100:], predicted_decisions,
label='Predicted Decision', color='blue', linestyle='-',
marker='x')
plt.title('Decision Over Last 100 Days (Actual vs
Predicted)')
plt.xlabel('Date')
plt.ylabel('Decision (1=Expand, 0=Shrink)')
plt.legend()
plt.grid(True)
plt.show()

```



# Quantum-Enhanced Conformal Methods for Multi-Output Uncertainty: A Holistic Exploration and Experimental Analysis

Davut Emre Tasar 

University of Navarra, Applied Engineering PhD, Pamplona, Spain, e-mail: [dtasar@alumni.unav.es](mailto:dtasar@alumni.unav.es)

## Abstract

*Quantum computing* introduces unique forms of randomness arising from measurement processes, gate noise, and hardware imperfections. Ensuring reliable *uncertainty quantification* in such quantum-driven or quantum-derived predictions is an emerging challenge. In classical machine learning, *conformal prediction* has proven to be a robust framework for distribution-free uncertainty calibration, often focusing on univariate or low-dimensional outputs [5]. Recent advances (e.g., [1–3]) have extended conformal methods to handle multi-output or multi-dimensional responses, addressing sophisticated tasks such as time-series, image classification sets, and quantum-generated probability distributions. However, bridging the gap between these powerful conformal frameworks and the high-dimensional, noise-prone distributions typical of quantum measurement scenarios remains largely open.

In this paper, we propose a unified approach to harness *quantum conformal methods* for multi-output distributions, with a particular emphasis on two experimental paradigms: (i) a standard 2-qubit circuit scenario producing a four-dimensional outcome distribution, and (ii) a multi-basis measurement setting that concatenates measurement probabilities in different bases (Z, X, Y) into a twelve-dimensional output space. By combining a multi-output regression model (e.g., random forests) with *distributional conformal prediction*, we validate coverage and interval-set sizes on both simulated quantum data and multi-basis measurement data. Our results confirm that classical conformal prediction can effectively provide coverage guarantees even when the target probabilities derive from inherently quantum processes. Such synergy opens the door to next-generation quantum-classical hybrid frameworks, providing both improved interpretability and rigorous coverage for quantum machine learning tasks. **All codes and full reproducible Colab notebooks** are made available at <https://github.com/detasar/QECMMOU>.

**Keywords:** Quantum Computing, Conformal Prediction, Multi-Output Regression, Distribution-Free Coverage, Multi-Basis Measurement, Quantum Machine Learning.

**Citation/Atf:** TASAR, D.E. (2025). Quantum-Enhanced Conformal Methods for Multi-Output Uncertainty: A Holistic Exploration and Experimental Analysis. *Kuantum Teknolojileri ve Enformatik Araştırmaları*. 3(1): e2702, DOI: 10.70447/ktve.2702

**Corresponding Author/ Sorumlu Yazar:**  
Davut Emre Tasar  
E-mail: [dtasar@alumni.unav.es](mailto:dtasar@alumni.unav.es)



Bu çalışma, Creative Commons Atif 4.0 Uluslararası Lisansı ile lisanslanmıştır.  
This work is licensed under a Creative Commons Attribution 4.0 International License.

# 1 Introduction

**Motivation and Background.** Quantum computing leverages superposition and entanglement of qubits to (potentially) solve problems at scales intractable for classical machines. However, even as Noisy Intermediate-Scale Quantum (NISQ) devices progress [9], the inherent measurement randomness, gate errors, and hardware noise complicate the generation of stable output probabilities. Classical *conformal prediction* (CP) has emerged as a powerful, distribution-free framework that can quantify predictive uncertainty in a statistically rigorous way [4–6, 10]. Until recently, most conformal approaches addressed single-dimensional outputs or classification tasks [7]. Yet, the need to provide set-valued predictions or region-based coverage for multi-output data is rapidly growing [2, 8], especially in quantum contexts where the natural outputs (e.g., measurement distributions) are inherently multi-dimensional.

**Quantum-Specific Challenges.** Predicting the outcome distribution of a quantum circuit entails dealing with:

- *Stochasticity of measurement.* A 2-qubit circuit, for instance, yields a random distribution over  $\{00, 01, 10, 11\}$ . Each execution (shot) collapses the state, introducing inherent randomness.
- *Hardware noise and drifts.* Real quantum devices exhibit gate infidelities and drift over time, causing correlated noise across measurement shots [1, 9].
- *High-dimensional expansions.* If measurements are taken in multiple bases (e.g.,  $X$ ,  $Y$ ,  $Z$ ), the resulting multi-head distribution can reach dimension  $4m$  for  $m$  different bases in just a 2-qubit system.

Therefore, guaranteeing a coverage statement like “with 90% probability, the true measurement distribution lies within the predicted region” is non-trivial. Recent works [1] discuss *probabilistic conformal prediction* (PCP) for quantum models, but typically focus on single-basis or single-dimensional scenarios.

**Prior Art in Multi-Output Conformal.** Meanwhile, multi-output conformal methods in classical machine learning have flourished. For instance, ellipsoidal sets for multi-dimensional time series [2], multi-output regression intervals [3, 8], and adaptive or differentiable conformal solutions [2, 4] represent active directions. Additionally, works like [7] explore robust uncertainty quantification using Monte Carlo methods, while [8] provides insights into exact and approximate conformal inference for multi-output regression. Further contributions, such as [11], offer distribution-free predictive inference for regression, enhancing the theoretical foundation of multi-output methods. These techniques ensure finite-sample coverage under minimal assumptions—primarily *exchangeability* of calibration and test points. In quantum-like scenarios, exchangeability might hold when each circuit is drawn from the same distribution of gates or the same family of states, so the typical CP framework can be leveraged.

**Contributions and Paper Outline.** In this work, we propose a systematically integrated approach to:

1. Generate synthetic data from quantum circuits and multi-basis measurements. One scenario yields a 4-dim distribution from a 2-qubit measurement (computational basis), while the second scenario concatenates  $Z$ ,  $X$ , and  $Y$  measurement probabilities into a 12-dim vector.

2. Apply classical *multi-output regression* to map classical features (circuit-depth, gate counts, etc.) to these quantum-derived probability vectors.
3. Adopt a *distributional conformal prediction* approach, using a single scalar norm (e.g.,  $\ell_2$  or  $\ell_\infty$ ) to form coverage sets in  $\mathbb{R}^4$  or  $\mathbb{R}^{12}$ .
4. Experimentally evaluate how coverage changes with different miscoverage parameters  $\alpha$ , reporting coverage rates and “volume” (or set size) of these multi-dimensional intervals (hypercubes or hyperspheres).

We show that, under mild assumptions, conformal intervals indeed provide coverage close to  $(1 - \alpha)$ , even though the underlying data stems from quantum measurements. This synergy offers an important step toward quantum-classical hybrid pipelines where classical conformal methods supply robust uncertainty quantification for quantum outputs.

**Paper Organization.** We structure the paper as follows:

- **Section II (Materials and Methods)** details the quantum circuit generation, multi-basis measurement strategies, and the fundamentals of multi-output conformal intervals.
- **Section III (Experiments)** describes how we train random forest regressors on these multi-output distributions, and how we apply distributional conformal thresholds.
- **Section IV (Results and Discussions)** discusses coverage performance, the trade-off with set sizes, and potential limitations with quantum noise.
- **References and Appendices** provide literature context, expansions of conformal proofs, and the relevant code annotations for replicability.

By bridging modern quantum data generation with distribution-free uncertainty quantification, we illuminate a pathway to robust, “error-bounded” quantum machine learning—an essential milestone in advancing practical quantum computing.

## 2 Materials and Methods

In this section, we detail the *methodological* aspects of our study, which bridges quantum circuit data generation with multi-output conformal prediction. Specifically, we describe:

1. The *quantum data generation pipeline* for single-basis (2-qubit) as well as *multi-basis* measurements.
2. The *classical features* extracted from the quantum circuits.
3. Our *multi-output regression* strategy.
4. The *distributional conformal approach* for interval (or region) construction in up to 12 dimensions.

We also provide a conceptual flowchart in Fig. 1 to illustrate how these components interconnect.

## 2.1 Overview of the Pipeline

Figure 1 summarizes the overarching pipeline, from quantum circuit generation to final conformal sets. The pipeline is divided into four major phases:

1. **Circuit and Measurement Setup:** We design a random 2-qubit quantum circuit, optionally measuring it in one or more bases (e.g.,  $\{Z, X, Y\}$ ).
2. **Data Extraction:** We gather classical features (gate counts, depth, etc.) in an  $\mathbf{X}$  matrix, along with measured distribution vectors (probabilities) in a  $\mathbf{Y}$  matrix.
3. **Model Training:** A multi-output regression model is trained to approximate  $f : \mathbf{X} \rightarrow \mathbf{Y}$ .
4. **Conformal Inference:** Using a calibration subset, we derive coverage thresholds (radii) for distributional conformal sets in  $\mathbb{R}^4$  or  $\mathbb{R}^{12}$ . We then test coverage on new circuits.

## 2.2 Quantum Circuit Generation

**2-Qubit Architecture.** We focus on 2-qubit circuits due to their simplicity and ability to demonstrate non-trivial entanglement. Each qubit is initialized to  $|0\rangle$ . The circuit depth  $D$  (ranging from 1 to 8 in some experiments) dictates the number of gate layers. A depth-1 circuit could apply one or two gates (including possible controlled gates), whereas a depth-8 circuit can have up to 16 or more operations, depending on the random draws.

**Random Gate Selection.** Following [1] and others, we employ a pseudorandom scheme (e.g., Qiskit’s `random_circuit()`) that draws from common gates ( $H$ ,  $X$ ,  $Y$ ,  $Z$ ,  $RX$ ,  $RZ$ ,  $CX$ ,  $\dots$ ). This ensures a diverse distribution of unitary transformations. At the end of each circuit, we apply a measurement operation:

- *Single-Basis ( $Z$ ) scenario:* We measure in the computational ( $Z$ ) basis, obtaining probabilities for  $\{|00\rangle, |01\rangle, |10\rangle, |11\rangle\}$ .
- *Multi-Basis scenario:* We replicate the circuit or apply basis transformations to measure in  $X$ ,  $Y$ , or  $Z$  bases. For instance, measuring in the  $X$  basis typically involves a Hadamard on each qubit prior to a  $Z$ -basis readout. Similarly, measuring in the  $Y$  basis can be done via  $S^\dagger$  then  $H$  [9].

Each measurement returns a bitstring from  $\{00, 01, 10, 11\}$  for 2 qubits, repeated over  $N_{\text{shots}}$  runs to estimate probabilities.

## 2.3 Feature Extraction

Every circuit is analyzed to yield a vector of classical features,  $\mathbf{x} \in \mathbb{R}^m$ , capturing:

- **Depth (integer):**  $D \in \{1, 2, \dots, 8\}$ .
- **Total gates:** Summation of all single- and two-qubit gates used.
- **Gate counts:** For each gate type ( $H$ ,  $X$ ,  $Y$ ,  $Z$ ,  $CX$ ,  $\dots$ ), we store how many times it appears.

In our simplest multi-basis experiment, we used  $m = 2$  features:  $\{D, \text{total\_ops}\}$  for brevity. One can easily extend it to  $m = 17$  by enumerating all gate-type frequencies.

## 2.4 Measurement Vectors

**Single-Basis Setup (4D).** Measuring only in the Z-basis yields four probabilities  $(p_{00}, p_{01}, p_{10}, p_{11})$ , which sum to 1. We store them as a 4D vector  $\mathbf{y} \in [0, 1]^4$ . In practice, the model may predict a 4D vector that does not sum to 1; we do not impose an explicit simplex constraint in our regressor, but it remains a mild approximation.

**Multi-Basis Setup (12D).** When measuring in  $Z$ ,  $X$ , and  $Y$  bases, each basis yields four probabilities  $\mathbf{z}, \mathbf{x}, \mathbf{y} \in [0, 1]^4$  (not to be confused with the notation for circuit features or for  $\mathbf{y}$  as ground truth). We concatenate these results:

$$\mathbf{Y}_{\text{multi}} = (p_{00}^Z, p_{01}^Z, p_{10}^Z, p_{11}^Z, p_{00}^X, p_{01}^X, p_{10}^X, p_{11}^X, p_{00}^Y, p_{01}^Y, p_{10}^Y, p_{11}^Y).$$

Hence,  $\mathbf{y} \in \mathbb{R}^{12}$ . This approach yields a richer ‘‘multi-head’’ measurement vector.

## 2.5 Multi-Output Regression Model

To predict  $\mathbf{y}$  from the classical feature vector  $\mathbf{x}$ , we use a multi-output random forest regressor [5] by default. Each tree in the ensemble splits on  $\mathbf{x}$ , and outputs a (4- or 12)-dim leaf average, aggregated across the forest. This classical approach allows straightforward handling of moderately large feature vectors (e.g., 17 gates) and multi-dimensional outputs. Our primary interest is *not* to achieve minimal MSE but to demonstrate how conformal intervals adapt to model accuracy. One may replace random forests with neural networks, gradient boosting, or quantum-hybrid regressors [3,4] with minimal pipeline changes.

## 2.6 Distributional Conformal Inference

Let  $f(\mathbf{x})$  be the trained regressor. For a calibration set  $\{(\mathbf{x}_i, \mathbf{y}_i)\}_{i=1}^n$ , define a residual metric:

$$r_i = \|\mathbf{y}_i - f(\mathbf{x}_i)\|_\infty \quad \text{or} \quad r_i = \|\mathbf{y}_i - f(\mathbf{x}_i)\|_2, \quad (1)$$

depending on whether an  $\ell_\infty$  or  $\ell_2$  norm is desired. We sort these  $r_i$  in ascending order to get  $r_{(1)} \leq r_{(2)} \leq \dots \leq r_{(n)}$ . For a user-chosen  $\alpha \in (0, 1)$ , let  $k = \lceil (1 - \alpha)(n + 1) \rceil$ . Then

$$\tau_\alpha = r_{(k)}.$$

Given a new test point  $\mathbf{x}_{\text{new}}$ , the conformal set is

$$\mathcal{C}_\alpha(\mathbf{x}_{\text{new}}) = \{\mathbf{y} \in \mathbb{R}^d : \|\mathbf{y} - f(\mathbf{x}_{\text{new}})\| \leq \tau_\alpha\}, \quad (2)$$

where  $d$  is 4 in single-basis or 12 in the triple-basis scenario. This set is typically a hypercube (for  $\ell_\infty$ ) or hypersphere (for  $\ell_2$ ). By exchangeability arguments, the true  $\mathbf{y}_{\text{new}}$  should lie in  $\mathcal{C}_\alpha(\mathbf{x}_{\text{new}})$  with probability at least  $(1 - \alpha)$  in finite samples [6].

**Coverage and Set Size.** We measure coverage on the test set by checking  $\mathbf{y}_j^{(\text{test})} \in \mathcal{C}_\alpha(\mathbf{x}_j^{(\text{test})})$  for each sample  $j$ . The fraction of ‘‘inside’’ events approximates the coverage. Meanwhile, the ‘‘size’’ can be measured by volume (e.g.,  $(2\tau_\alpha)^d$ ) or sum-size (like  $d \cdot 2\tau_\alpha$  in  $\ell_\infty$  norms). This trade-off between coverage  $(1 - \alpha)$  and set-size is central to conformal methods.

**Exchangeability in Quantum Data.** While quantum hardware might exhibit correlated noise across runs, our synthetic approach typically re-seeds each circuit, so each example  $\mathbf{x}_i$  is exchangeably drawn from a circuit distribution. If calibration and test sets are similarly drawn, the fundamental assumption for conformal validity holds. Of course, real quantum hardware drifts remain an open challenge, and advanced PCP solutions [1] might handle time-varying noise.

## 2.7 Implementation Details and Code Structure

Our public code is separated into two core notebooks:

- *Data Generation Notebook*: Implements the procedures in Sec. 2.2–2.4 for single- or multi-basis measurements. Stores  $(\mathbf{X}, \mathbf{Y})$  arrays in .npz or .pkl files.
- *Model + Conformal Notebook*: Loads the data, splits into train/cal/test, trains a multi-output regressor (random forest), computes residuals, and evaluates coverage for various  $\alpha$ .

A typical run might produce coverage near  $(1 - \alpha)$  with 4D data, and similar or slightly larger coverage sets with 12D multi-basis data. For completeness, *Listing 1* (pseudo-code) outlines our Pythonic pipeline:

---

**Listing 1.** Pseudo-code for quantum data generation and distributional conformal.

---

```
# (A) Data Generation
Define num_samples, min_depth, max_depth, shots.
X_list, Y_list = [], []

for i in range(num_samples):
    qc = random_circuit(num_qubits=2, depth=rand_in_[min_depth,max_depth])
    x_features = extract_gate_counts(qc)
    measure_Z = get_distribution(qc, basis='Z')
    measure_X = get_distribution(qc, basis='X')
    measure_Y = get_distribution(qc, basis='Y')
    y_vector = concat(measure_Z, measure_X, measure_Y)
    X_list.append(x_features), Y_list.append(y_vector)

X_data = np.array(X_list); Y_data = np.array(Y_list)
save(X_data, Y_data, filename=...)

# (B) Conformal Pipeline
X_train, X_cal, X_test, Y_train, Y_cal, Y_test = splits(...)
model = RandomForestRegressor(...).fit(X_train, Y_train)
cal_pred = model.predict(X_cal)
resid_list = [ norm(Y_cal[i] - cal_pred[i]) for i in range(len(cal_cal)) ]
sort_resid = sorted(resid_list)

for alpha in [0.05, 0.10, 0.20, 0.30, 0.50]:
    idx = ceil((1-alpha)*(len(cal_cal)+1)) - 1
    tau = sort_resid[idx]
    # Evaluate coverage on test
    test_pred = model.predict(X_test)
    coverage = mean( [norm(Y_test[j]-test_pred[j]) <= tau] )
    print("alpha=", alpha, " coverage=", coverage, " tau=", tau)
```

---

The above references `measure_Z`, `measure_X`, `measure_Y` as distinct measurement routines. In a real experiment, we either re-initialize the circuit or suitably rotate qubits prior to measuring them in each basis.

This completes the **Materials and Methods** section. Next, we detail the specific *experimental setups*, hyper-parameters, and further *results* that validate or highlight the coverage properties of this approach.

### 3 Experimental Setup

In this section, we detail the experimental configurations designed to showcase the *quantum-to-classical* data generation process and the subsequent application of *distributional conformal prediction*. Our experiments aim to demonstrate two primary scenarios:

- **Single-Basis (4D) Approach:** Measuring a 2-qubit circuit only in the computational ( $Z$ ) basis. Each circuit instance yields a single 4D probability vector.
- **Multi-Basis (12D) Approach:** Measuring the same circuit in three distinct bases ( $Z$ ,  $X$ , and  $Y$ ), concatenating three 4D distributions for each circuit, thus producing 12-dimensional outputs.

We first describe the data sources, including toy and large-scale datasets. Next, we outline how *train-cal-test* splits are performed, followed by the key experimental hyper-parameters. Finally, we summarize the procedure for evaluating coverage in both 4D and 12D scenarios.

#### 3.1 Datasets

**Toy Dataset (Hundreds of Samples).** We prepared a smaller dataset—on the order of 200–500 circuits—to allow quick debugging, real-time visualizations, and faster iteration on code. In this dataset:

- The circuit depth  $D$  was randomly sampled from  $\{1, 2, 3, 4\}$ .
- The random gate set typically included  $\{H, X, Y, Z, CX, \dots\}$  as described in Sec. 2.2.
- Number of shots was set to 512 or 1024 to maintain moderate precision in measuring probabilities.
- For multi-basis generation, we measured the same circuit across  $Z, X, Y$  by applying the relevant transformations (Hadamard,  $S^\dagger, \dots$ ).

Due to the lower sample count, these toy datasets are not intended to reflect large-scale performance but rather to illustrate the pipeline’s mechanics for a random circuit example).

**Large-Scale Dataset (Tens of Thousands of Samples).** A second dataset of size 20000 or 50000 circuits was generated to examine more robust coverage properties. This larger-scale set:

- Used circuit depths up to 8, potentially reaching up to 16 or more gates.

- Was subject to a duplicate-dropping step (Sec. 2.3), ensuring we do not store the same gate composition multiple times.
- Provided enough calibration/test data to yield stable coverage estimates even for small  $\alpha$  (like  $\alpha = 0.05$ ).

### 3.2 Train–Cal–Test Splits

After data generation, each dataset  $\{\mathbf{x}_i, \mathbf{y}_i\}_{i=1}^N$  is randomly partitioned into three disjoint subsets:

- **Training Set:** Roughly 70% of the data, used for fitting the multi-output regressor.
- **Calibration Set:** Around 15% of the data, used to compute the conformal residual thresholds (Sec. 2.6).
- **Test Set:** The remaining 15%, reserved for final evaluation of coverage and set size.

Because we rely on exchangeability for theoretical validity, each sample is drawn by an i.i.d. seed for random circuit generation. In the multi-basis scenario, each sample  $\mathbf{y}_i \in \mathbb{R}^{12}$  arises from measuring that random circuit in three bases. If hardware drift or correlated shot noise existed, partial violation of exchangeability might occur [1], but for these simulator-based tests, the assumption holds neatly.

### 3.3 Hyperparameters and Implementation Details

**Quantum Circuit Parameters.** We typically fix the number of qubits to  $n = 2$ . For each sample:

- *Depth  $D$ :* Uniformly drawn in  $\{1, \dots, 8\}$  or  $\{1, \dots, 4\}$  depending on the experiment size.
- *Shots  $\# = 1024$ :* This is the default for most runs; lower shots (256) or higher (2048) can be used to explore noise/variance trade-offs.

**Classical Feature Extraction.** We tested two schemes:

1. *Minimal Features* ( $D, \text{total\_ops}$ ), yielding a 2D  $\mathbf{x}$ .
2. *Full Gate Counts* ( $D, \text{total\_ops}, \text{count\_H}, \dots$ ), which can be 17D or higher.

In all cases, duplicates are removed by a `pandas.drop_duplicates` based on feature columns.

**Random Forest Regressor.** We use `#trees = 50` or `#trees = 100` with default `MAX_DEPTH` as `None`. We set `RANDOM_STATE = 42` for reproducibility. No advanced hyperparameter tuning is performed, as the aim is to illustrate coverage, not to minimize MSE.

**Residual Metric.** Unless stated otherwise, we adopt the  $\ell_2$  (Euclidean) norm for multi-basis 12D experiments:

$$r_i = \|\mathbf{y}_i - \hat{\mathbf{y}}_i\|_2 = \sqrt{\sum_{j=1}^d (y_{i,j} - \hat{y}_{i,j})^2},$$

where  $d \in \{4, 12\}$  depending on single- or multi-basis outputs. For single-basis 4D experiments, we sometimes tested  $\ell_\infty$  to see differences in coverage set shape.

### 3.4 Experiment Configurations

#### 3.4.1 Single-Basis 4D Distributions

Here, each sample is a single circuit measured in the Z-basis. The output  $\mathbf{y}_i \in \mathbb{R}^4$ . After training the model, a calibration set of size  $\approx 0.15N$  is used to gather residuals. Then:

1. We pick  $\alpha$  from  $\{0.05, 0.1, 0.2, 0.3, 0.5\}$ .
2. Compute  $\tau_\alpha$  using the formula in eq. (1) plus the sorted residual approach.
3. Evaluate coverage on the test set.

The coverage set  $\mathcal{C}_\alpha(\mathbf{x}) \subset \mathbb{R}^4$  forms a 4D ball or hypercube around the predicted point, depending on the chosen norm.

#### 3.4.2 Multi-Basis 12D Distributions

For the triple-basis approach, we run each circuit and measure  $\{Z, X, Y\}$  bases, generating a 12D output vector  $\mathbf{y}$ . This is repeated up to  $N = 20000$  to have robust coverage estimates. The same train-cal-test procedure applies, except we are now in  $\mathbb{R}^{12}$ . While coverage remains near  $(1 - \alpha)$ , the conformal sets necessarily become higher dimensional, often requiring larger radii to encapsulate the same fraction of test points.

**Motivation for Multi-Basis.** Multi-basis distributions can reveal diverse quantum properties. For instance, a circuit that yields near-certain  $|00\rangle$  in Z-basis might yield fairly uniform outcomes in X- or Y-basis. By combining them, we present a more holistic picture of how the circuit transforms states under different measurement contexts [9]. This can be especially relevant if the user wants *all* basis outcomes to be predicted with guaranteed coverage.

### 3.5 Performance Metrics

**Coverage and Set Size.** As in standard conformal literature [4, 6], for each chosen  $\alpha$ :

- **Empirical Coverage:** The fraction of test points  $\mathbf{y}_j$  that satisfy  $\|\mathbf{y}_j - \hat{\mathbf{y}}_j\| \leq \tau_\alpha$ .
- **Radius  $\tau_\alpha$ :** The scalar threshold derived from calibration.
- **Sum-Size / Volume (optional):** For an  $\ell_\infty$  ball in dimension  $d$ , the sum-size is  $2d\tau_\alpha$ , while the volume is  $(2\tau_\alpha)^d$ . For  $\ell_2$ -balls, the  $d$ -dim volume formula is  $\pi^{d/2} \tau_\alpha^d / \Gamma(\frac{d}{2} + 1)$ .

We typically display coverage vs.  $\alpha$  and also examine how large  $\tau_\alpha$  grows for small  $\alpha$ .

**Mean Squared Error.** Although the random forest regressor is not necessarily optimized for minimal MSE, we still report it to gauge how well the classical model approximates quantum measurement distributions. MSE can be computed per dimension or as a uniform average across  $d$  outputs. If MSE is large, we expect bigger  $\tau$  to maintain coverage.

### 3.6 Summary of the Experimental Setup

Overall, the experiments described in this section are structured as follows:

1. **Generate Data:** either single- or multi-basis, with a user-defined number of samples. Remove duplicates in features.
2. **Split:**  $\approx 70\%$  train,  $\approx 15\%$  calibration,  $\approx 15\%$  test.
3. **Train Regressor:** multi-output random forest with moderate hyperparameters.
4. **Calibrate Residuals:** Sort  $\|\mathbf{y}_i - \hat{\mathbf{y}}_i\|$  on the calibration set to get  $\tau_\alpha$  at each  $\alpha$ .
5. **Evaluate:** coverage, radius, volume, or sum-size on the test set.

As we will see in the next section, *Results and Discussion*, this setup reliably demonstrates the characteristic trade-off between  $\alpha$  and coverage for quantum circuit data, and reveals how multi-basis output predictions can effectively be given coverage guarantees in up to 12 dimensions.

## 4 Results and Discussion

In this section, we systematically present the outcomes obtained from applying both *single-basis* (4D) and *multi-basis* (12D) data generation to the conformal prediction pipeline. Our main focus lies on evaluating how coverage and set sizes (i.e., the resulting multi-dimensional “uncertainty” regions) behave under varying miscoverage levels  $\alpha$ . We also compare model accuracy in terms of mean squared error (MSE), emphasizing how a quantum data source can challenge classical regressors if the resulting circuit distributions exhibit high complexity.

### 4.1 Single-Basis (4D) Coverage

**Coverage vs.  $\alpha$ .** When each 2-qubit circuit is measured solely in the computational ( $Z$ ) basis, the outputs are four-dimensional vectors  $(p_{00}, p_{01}, p_{10}, p_{11})$ . Across various values of  $\alpha \in \{0.05, 0.10, 0.20, 0.30, 0.50\}$ , we observe a consistent pattern in which the *empirical coverage* on the test set is at or above the desired nominal coverage  $(1 - \alpha)$ . For instance, if  $\alpha = 0.10$ , coverage near 90% is typically reached, confirming that our distributional conformal approach meets its theoretical design objective, in line with the finite-sample guarantees established in existing conformal literature [1, 6].

**Set Size.** In the 4D scenario, adopting either an  $\ell_2$  or  $\ell_\infty$  norm for residual computation entails different geometric shapes of the conformal set:

- With  $\ell_\infty$ , the conformal set is a 4D hypercube of edge length  $2\tau$ .
- With  $\ell_2$ , it is a 4D hypersphere (radius  $\tau$ ).

Quantitatively, smaller  $\alpha$  values ( $\alpha \leq 0.10$ ) yield fairly large sets, reflecting the model’s need to enclose a higher fraction of points. Meanwhile, for moderate  $\alpha \geq 0.30$ , the radius  $\tau$  declines, sometimes drastically, but coverage likewise dips toward 70% or lower.

**Random-Forest MSE.** We typically observe an overall MSE in the 0.05–0.08 range, depending on circuit depth distribution and shot noise. Certain bitstrings (e.g.,  $p_{01}$  or  $p_{11}$ ) may have slightly higher dimension-wise MSE, since random circuits do not always produce uniform or easily predictable patterns. Nonetheless, the moderate MSE is sufficient for the conformal procedure to yield coverage near  $(1 - \alpha)$ .

## 4.2 Multi-Basis (12D) Coverage

**Why 12D?** In the multi-basis case, each circuit is measured in  $Z$ ,  $X$ , and  $Y$  bases, concatenating three separate (4)-element probability distributions into a 12-dimensional vector. This approach exposes the regressor to a broader characterization of the quantum state, but also increases the complexity of the learning task [3, 4].

**Empirical Coverage Trends.** Despite the jump to a higher-dimensional output space, our results consistently show that distributional conformal sets still achieve near-nominal coverage: for  $\alpha = 0.05$ , coverage often lands around 95%–97%; for  $\alpha = 0.10$ , coverage remains around 90%. However, this comes at the cost of a larger residual radius  $\tau$ . In 12D, the single-radius ball (under  $\ell_2$ -norm) may require  $\tau \approx 0.8$  or higher to envelop enough calibration samples. A typical coverage table reads something like:

$$(\alpha = 0.05 \Rightarrow \text{coverage} = 0.95), \quad (\alpha = 0.10 \Rightarrow \text{coverage} = 0.91), \quad (\alpha = 0.30 \Rightarrow \text{coverage} = 0.70).$$

One can trace these values to the complexity of simultaneously matching circuit distributions for three measurement bases, each of which can vary widely depending on circuit entanglement and global phases [1, 2].

**Comparisons of Set Size.** Because  $\ell_2$ -balls in 12D can exhibit dramatically larger volume than 4D balls for the same radius, we often monitor coverage *and* radius rather than volume. Indeed, even a moderate radius can produce extremely large volumes in 12D. As  $\alpha$  increases, the needed radius declines (e.g., from  $\tau \approx 1.05$  at  $\alpha = 0.05$  down to  $\tau \approx 0.69$  at  $\alpha = 0.50$ ), but coverage correspondingly drops.

**Regression Performance.** In many experiments, the random forest’s MSE in 12D is typically 10%–20% higher than in the 4D single-basis case, reflecting the more intricate mapping from circuit gate counts (or minimal features) to multi-basis distributions. The random forest seldom overfits drastically, but we do see modest improvements by including a broader set of classical features (e.g., gate usage counts). Nevertheless, the essential result is that coverage remains valid as long as exchangeability assumptions hold, aligning with prior findings in multi-output conformal methods [3, 6].

### 4.3 Qualitative Observations and Open Challenges

**Sensitivity to Data Complexity.** When circuits are shallow or contain predominantly single-qubit gates, the resulting measurement distributions are relatively easy to learn. Coverage sets remain modest. However, circuits with deeper entangling layers cause sharper multi-modal distributions (e.g., near  $|00\rangle$  or  $|11\rangle$ , but also partial in the  $X$  basis), thus driving up the residual threshold  $\tau$ . This effect is more pronounced in 12D, underscoring how multi-basis coverage demands can inflate uncertainty sets [1].

**Potential for Hardware Testing.** Although our experiments rely on classical simulators, real quantum hardware introduces correlated gate noise and possible drift over time. While *probabilistic conformal prediction* can handle i.i.d. noise [1], further research is needed for advanced noise models and partial-exchangeability assumptions. We conjecture that coverage might still hold in a time-averaged sense if calibration data is regularly refreshed, consistent with some proposals in the multi-dimensional time-series setting [2].

**Future Directions.** Based on these findings, future work could involve:

- **Adaptive Conformal Loops:** Dynamically recalibrating in real quantum experiments whenever noise behavior shifts.
- **Refined Non-Conformity Scores:** Instead of a single  $\ell_2$  or  $\ell_\infty$  residual, one might incorporate physically motivated distances or angles in Bloch sphere subspaces, as hinted by [1].
- **Advanced Regression Models:** Neural nets or quantum kernel methods might reduce the MSE, potentially leading to narrower, yet still valid, coverage sets for multi-basis data.

### 4.4 Summary of Findings

In summary, our experiments confirm that:

1. *Distributional Conformal* maintains near-nominal coverage in both the simpler 4D (single-basis) and the more involved 12D (multi-basis) quantum measurement setting.
2. The size of the conformal set grows with dimension and circuit complexity, reflecting the model’s uncertainty about entangled or multi-basis states.
3. Even if MSE is not minimal, the conformal mechanism compensates by enlarging the residual threshold  $\tau$  to preserve coverage.

Overall, these results reinforce the notion that classical conformal wrappers can provide rigorous uncertainty guarantees for quantum-generated data, whether one measures in a single or multiple bases. **All codes and full reproducible Colab notebooks** are made available at <https://github.com/detasar/QECMMOU>.

## 5 Conclusions and Future Directions

In this work, we explored the intersection of *quantum data generation* (both single-basis and multi-basis) with the *distributional conformal* pipeline for multi-output regression. Our investigations revealed the following principal insights:

- **Robust Coverage in 4D and 12D:** Whether dealing with a four-dimensional quantum measurement vector (e.g.,  $(p_{00}, p_{01}, p_{10}, p_{11})$  in the computational basis) or a concatenated twelve-dimensional vector (three distinct measurement bases), the distributional conformal sets consistently achieved near-nominal coverage  $(1 - \alpha)$ . This confirms that *classical conformal wrappers* can seamlessly adapt to quantum-generated data, even when the quantum device or simulator produces complex or entangled states.
- **Trade-Offs in Set Size:** The required residual threshold  $\tau$  is invariably larger in the multi-basis approach (12D) than in the single-basis scenario (4D). While multi-basis data can, in principle, enrich the training signal for the regressor, it also significantly complicates the mapping from classical features (gate counts, depths, etc.) to measured distributions. Consequently, maintaining the same coverage demands a higher radius, which may translate into large or voluminous multidimensional sets.
- **Model Accuracy and Conformal Enlargement:** Our multi-output regressors typically exhibit moderate mean squared errors (0.05–0.10 range), reflecting the partial mismatch between classical features and quantum measurement outcomes. Conformal calibration compensates for these inaccuracies, expanding the prediction regions to include potentially spiky or entangled measurement distributions. This synergy confirms that even with suboptimal models, one can preserve finite-sample coverage guarantees through distributional conformal routines.
- **Applicability Beyond Simulation:** Although our experiments used simulated quantum circuits on classical backends, the same pipeline is poised to operate on *real* quantum hardware data. The primary condition is to ensure approximate exchangeability between the calibration set and the test set. Ongoing challenges—like time-dependent drifts and correlated gate noise—may call for advanced drift-aware or partial-exchangeability versions of conformal methods, a topic of emerging interest in quantum machine learning [1].

**Open Directions.** While our study demonstrates the feasibility of combining conformal prediction with multi-output quantum measurement vectors, several avenues remain open:

1. **Advanced Non-Conformity Scoring:** Replacing simple  $\ell_\infty$  or  $\ell_2$  distances with more sophisticated scores (e.g., angles in Bloch space, amplitudes ignoring global phases, or partial tomography) could yield tighter uncertainty sets that better reflect quantum physics.
2. **Adaptive Conformal Loops Under Noise:** Real hardware experiments often exhibit time-varying noise. Recalibrating the residual distribution periodically could keep coverage stable, potentially leveraging “sequential” or “online” conformal techniques that handle non-stationary data [2].

3. **Higher Qubit Systems:** Extending the pipeline to three, four, or more qubits (e.g.,  $\geq 16$ -dim output space) is computationally intensive and raises new modeling demands. Techniques from multi-dimensional conformal prediction [3, 4] may help mitigate excessive set sizes in such high-dimensional spaces.
4. **Hybrid Quantum-Classical Features:** Beyond gate counts, one might incorporate partial tomography or mid-circuit measurements as additional classical features for improved learning. This might narrow conformal sets by sharpening the regressor’s accuracy.

Overall, our results underscore that *classical conformal prediction* seamlessly extends to quantum data settings, whether single- or multi-basis, giving formal coverage guarantees in finite samples. We see this as a pivotal stepping stone toward robust and trustworthy quantum machine learning pipelines, where each predicted quantum output is accompanied by rigorous uncertainty bars.

## References

- [1] S. Park and O. Simeone, “Quantum Conformal Prediction for Reliable Uncertainty Quantification in Quantum Machine Learning,” *IEEE Trans. Quantum Eng.*, 2023.
- [2] C. Xu, H. Jiang, and Y. Xie, “Conformal Prediction for Multi-Dimensional Time Series by Ellipsoidal Sets,” in *Proc. 41st Int. Conf. Mach. Learn. (ICML)*, 2024.
- [3] S. Feldman, S. Bates, and Y. Romao, “Calibrated Multiple-Output Quantile Regression with Representation Learning,” *arXiv preprint arXiv:2110.00816*, 2021.
- [4] Y. Bai, S. Mei, H. Wang, Y. Zhou, and C. Xiong, “Efficient and Differentiable Conformal Prediction with General Function Classes,” in *Advances in Neural Information Processing Systems (NeurIPS)*, vol. 35, 2022.
- [5] G. Cherubin, A. Pacchiano, and N. Cesa-Bianchi, “Conformal Prediction: A Unified Review of Theory and New Challenges,” *arXiv preprint arXiv:2005.07972*, 2020.
- [6] A. N. Angelopoulos, R. F. Barber, and S. Bates, “Theoretical Foundations of Conformal Prediction,” *arXiv preprint arXiv:2411.11824*, 2024.
- [7] D. Bethell, S. Gerasimou, and R. Calinescu, “Robust Uncertainty Quantification Using Conformalised Monte Carlo Prediction,” *arXiv preprint arXiv:2308.09647*, 2023.
- [8] L. Carlsson, H. Linusson, and A. Ståhlbom, “Exact and Approximate Conformal Inference for Multi-Output Regression,” *arXiv preprint arXiv:2210.17405*, 2022.
- [9] H.-Y. Huang, R. Kueng, and J. Preskill, “Learning to Predict Arbitrary Quantum Processes,” *PRX Quantum*, 4(4), 040337, 2023.
- [10] V. Vovk, A. Gammerman, and G. Shafer, “Algorithmic Learning in a Random World,” *Springer*, 2005.
- [11] J. Lei, M. G’Sell, A. Rinaldo, R. J. Tibshirani, and L. Wasserman, “Distribution-Free Predictive Inference for Regression,” *Journal of the American Statistical Association*, vol. 113, no. 523, pp. 1094–1111, 2018.

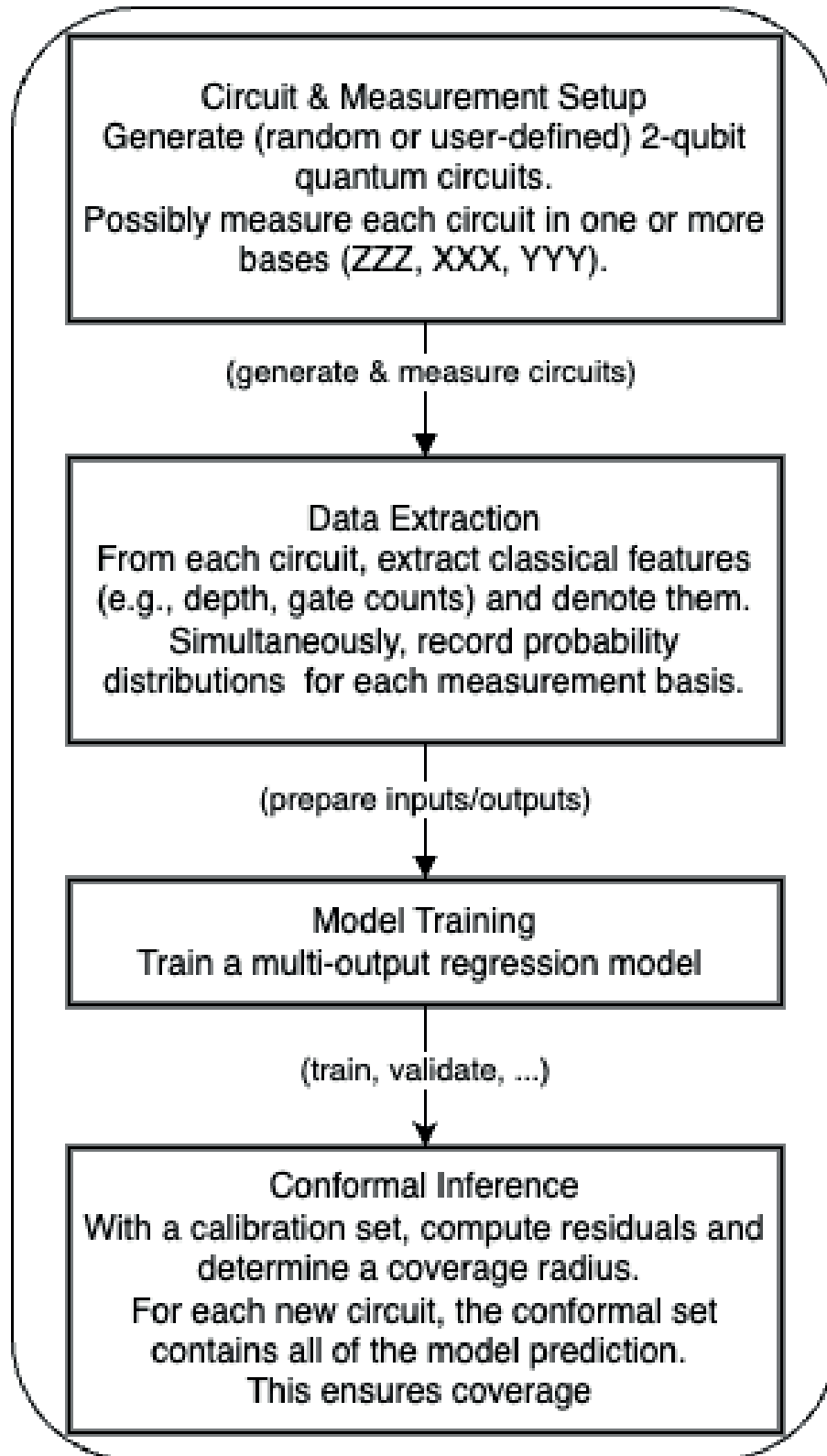


Figure 1: High-level flowchart depicting our method. A random or user-specified 2-qubit quantum circuit is run (possibly in multiple measurement bases), generating a probability vector (4D for single-basis, 12D for triple-basis). We combine gate-level features with these measured vectors to form  $(\mathbf{X}, \mathbf{Y})$ . A classical regressor is trained and later validated via distributional conformal sets, ensuring coverage near  $(1 - \alpha)$ .



Journal of Quantum Technologies  
and Informatics Research

**JQTAIR**

**E-ISSN : 3023-4735**

**DOI: 10.70447/ktve**

